EXTRACELLULAR VESICLE-ASSOCIATED DNA IN NEUROBLASTOMA:

HITCHING A RIDE FOR TUMOUR PROGRESSION?

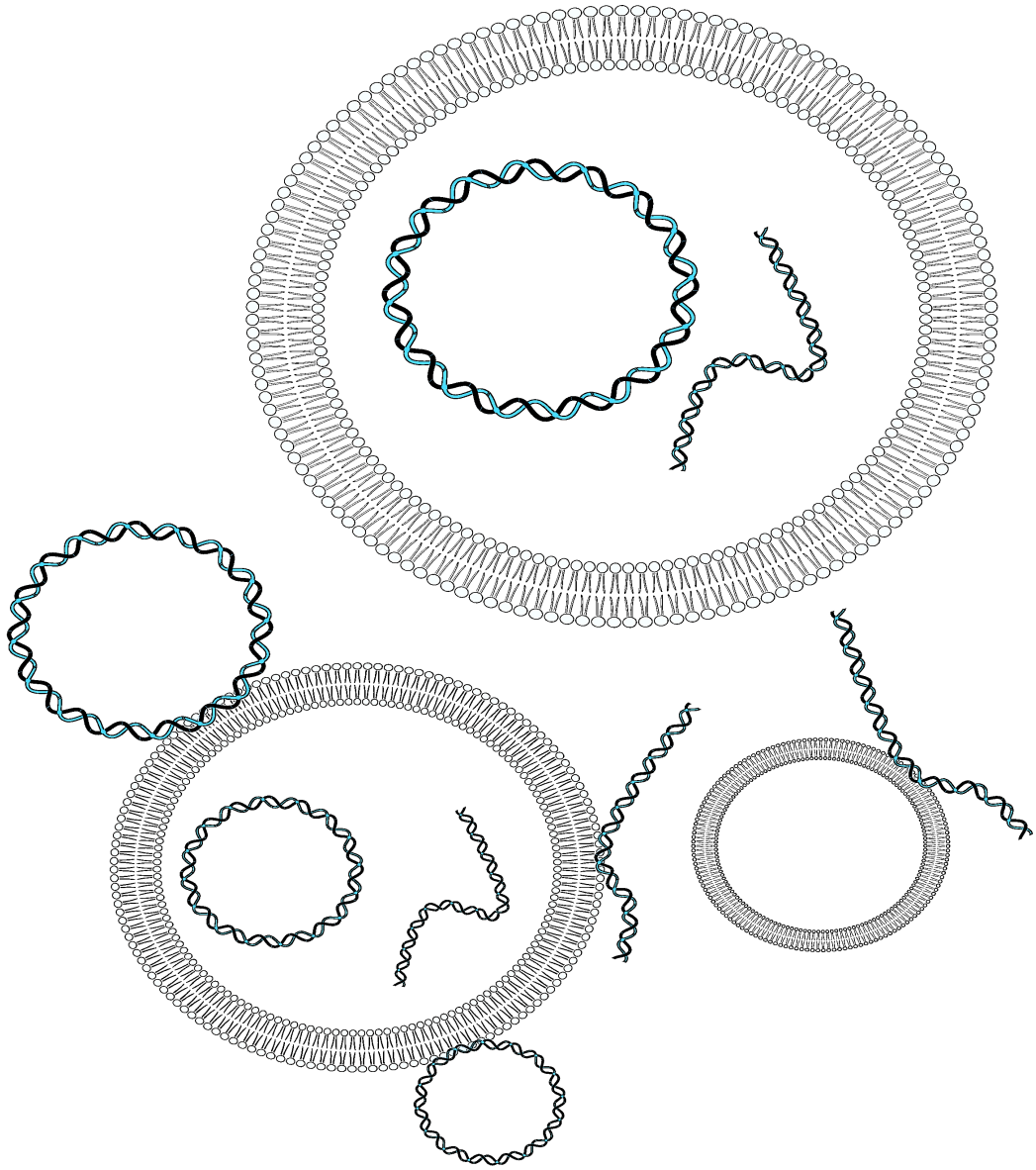

RICK TIMMERIJE

UNIVERSITY OF TWENTE. | TECHMED CENTRE

BioElectric signaling and Engineering

Extracellular vesicle-associated DNA in neuroblastoma: Hitching a ride for tumour progression?

Rick Timmerije

Enschede, January 12, 2024

Research conducted as a graduation project for the master's degree program of Biomedical Engineering

University of Twente

Graduation Committee

prof.dr. A. Kocer
(Committee chair, Bioelectric signalling and engineering, University of Twente)

prof.dr.ir. J. Huskens
(Molecular nanofabrication, University of Twente)

dr. K. Broersen
(Applied Stem Cell Technology, University of Twente)

S. Taschner-Mandl, PhD
(St. Anna Children's Cancer Research Institute, Vienna, Austria)

Contents

Abstract

Introduction: Neuroblastoma, a prevalent and aggressive pediatric cancer originating from immature nerve cells in the sympathetic nervous system, poses significant challenges despite advancements in treatment. Recent studies highlight the role of extrachromosomal DNA (ecDNA) associated with extracellular vesicles (EVs) in neuroblastoma, particularly its association with oncogene amplification, tumour progression and drug resistance. While a further need for investigation is recognised, this study outlines three key research goals: (1) Investigate ecDNA morphology and quantity in the SHEP-2 neuroblastoma cell line using metaphase spreads. (2) Examine whether EVs released by SHEP-2 cells contain DNA and determine its location within or outside the vesicle. (3) Explore the transfer of EV-associated ecDNA between different cells.

Results: Visualization of ecDNA in SHEP-2 cells, despite extensive optimisation of metaphase spreads of coverslip adherent cells, revealed challenges due to overlapping chromosomal fragments. Significant quantities of DNA were found in EV isolation fraction with and without enzymatic digestion of non-enclosed DNA. This indicates the presence of DNA both inside and outside of EVs. With bioorthogonal metabolic labelling, the nuclear DNA of SHEP-2 cells was successfully labelled by incorporating F-ara-EdU and later 'clicking' a fluorophore to it using the CuAAC reaction. This could be used to follow the DNA from these cells when it is not known which genes are transferred, setting the stage for a subsequent detection and localization experiment for this DNA in EV fractions isolated using centrifugation and ultracentrifugation. However, the anticipated CuAAC click-labelling technique for detecting ecDNA from the isolated EV fraction in gel electrophoresis faced challenges. Next to this, the ecDNA from EV fractions isolated from bioorthogonal labelled SHEP-2 cell culture in different cell cultures could not be localized.

Conclusion and discussion: Despite extensive optimization of the metaphase spreads for the observation of ecDNA, the overlapping chromosomal fragments posed a significant challenge, making it difficult to distinguish individual chromosomes and hindering a clear observation of ecDNA. The investigation into EVs secreted by SHEP-2 cells revealed the presence of DNA in the EV fraction and suggested the existence of both free or vesicle-associated DNA and membrane-enclosed DNA within the EV isolation fraction. However, the EV yield and exclusion of non-EV material remain unknown. Efforts to explore ecDNA transfer in cases where the genes are unidentified involved the effective use of a bioorthogonal metabolic labelling strategy within cells adhering to coverslips. However, specific detection of ecDNA in the EV fraction remained inconclusive due to challenges such as fluorophore binding issues or a potential absence of ecDNA in the sample. The experiment designed to explore the transfer of ecDNA through EVs did not yield usable results but the experimental set-up can contribute to future investigations.

Keywords: Neuroblastoma; extrachromosomal DNA; ecDNA; extracellular vesicles; EVs;

1 Introduction

Neuroblastoma is a rare but aggressive paediatric cancer that arises from immature nerve cells in the sympathetic nervous system. It is the most common extracranial solid tumour in children, accounting for approximately 8 to 10% of all childhood cancers [1] and 15% of deaths related to cancer.[2, 3] Despite advances in treatment, the prognosis for high-risk neuroblastoma remains poor, with a five-year survival rate of less than 50%.[4]

Recent studies have shown that extrachromosomal DNA (ecDNA) is commonly found in neuroblastoma cells and plays a critical role in tumour progression and drug resistance.[5, 6] EcDNAs are circular DNA molecules that exist independently of the chromosomal DNA and can carry oncogenes or other cancer-relevant genes. They are generated through various mechanisms such as chromothripsis, telomere dysfunction, or replication stress.[7] The circular topology of ecDNAs leads to an open chromatin conformation and generates new gene regulatory interactions. This can result in increased expression of oncogenes and altered signalling pathways that promote tumour growth and survival.[8]

Amplification of the oncogene MYCN is one of the most common genetic alterations observed in neuroblastoma and is associated with poor prognosis.[9, 10] MYCN amplification has been shown to occur on ecDNAs, which can lead to increased expression of MYCN and altered signalling pathways that promote tumour growth and survival. MYCN overexpression in tumours is generated by a variety of processes, which suggests that other factors may contribute to the clinical heterogeneity observed in neuroblastoma.[11]

Recent studies have also shown that ecDNA can be found inside and on the surface of extracellular vesicles (EVs) released by cancer cells.[12] EVs are small membrane-bound particles that are secreted by cells and can contain various biomolecules such as proteins, lipids, and nucleic acids. They play a critical role in intercellular communication and can transfer genetic material between cells.[13] EcDNA-containing EVs have been shown to exist in various types of cancer, including neuroblastoma. These ecDNA-containing EVs can be taken up by neighbouring or distant cells, leading to the transfer of oncogenes or other cancer-relevant genes and the promotion of tumour growth and metastasis.[14, 15]

Furthermore, recent studies have suggested that ecDNA-containing EVs may also play a role in drug resistance. For example, it has been shown that EVs released by methotrexate-resistant neuroblastoma cells contain ecDNAs carrying the DHFR gene, which confers resistance to methotrexate. These ecDNA-containing EVs can be taken up by sensitive cells, leading to the transfer of DHFR and the acquisition of drug resistance.[7, 16]

Therefore, further investigation is needed to elucidate the molecular mechanisms underlying ecDNA quantity, distribution and their contribution to tumour heterogeneity and drug resistance. This study aims to (1) investigate ecDNA morphology and quantity of the SHEP-2, neuroblastoma cell line, (2) whether EVs secreted by these cells contain DNA and if this DNA is located inside or outside the vesicle and (3) if there is the transfer of EV-associated ecDNA between cell types. The ecDNA morphology and quantity are shown in metaphase spreads. Successively, the quantity, location and origin of EV-associated DNA are researched using differential centrifugation and bioorthogonal metabolic labelling strategies. The findings of this research may offer valuable insights that can be instrumental in further investigations concerning the influence of chemotherapy on both ecDNA and extracellular vesicle-associated DNA in neuroblastoma *in vitro* models.

2 Extrachromosomal DNA in neuroblastoma

2.1 Neuroblastoma

Neuroblastoma is a malignant tumour that arises from precursor cells of the sympathetic nervous system[17], typically occurring in young children (median age of 17 months).[18] It is the most common solid tumour in infants and the third most common paediatric malignancy, accounting for approximately 8 to 10% of all childhood cancers[1] and 15% of deaths related to cancer.[2, 3] Neuroblastoma exhibits a wide range of clinical behaviours, with some tumours spontaneously regressing or maturing into benign ganglioneuromas, while others can be highly aggressive and metastasize to distant sites.[17, 19]

The origin of neuroblastoma lies in the neural crest cells, a transient population of cells that give rise to various nervous system components during embryonic development.[20] Neuroblastoma can arise in any part of the sympathetic nervous system, but it most commonly arises in the adrenal glands, which are located above the kidneys. However, it can also occur in other sympathetic ganglia along the spine, neck, chest, or pelvis.[21, 22]

The clinical presentation of neuroblastoma can vary widely, depending on the location, stage, and biological characteristics of the tumour. Common signs and symptoms include a palpable abdominal mass, abdominal pain, weight loss, bone pain, fatigue, and, in advanced cases, features of catecholamine excess such as hypertension, tachycardia, and reduced facial flushing.[22] Diagnosis is typically based on a combination of clinical evaluation, imaging studies (such as computed tomography (CT) scans, magnetic resonance imaging (MRI), and metaiodobenzylguanidine (MIBG) scintigraphy), and histopathological examination of tumour tissue.[23, 24]

Neuroblastoma is a complex and heterogeneous disease with diverse genetic and molecular features, and its prognosis can vary greatly depending on several risk factors, including age at diagnosis, stage of disease, tumour histology, and genetic markers. In particular, neuroblastoma genetic mutations and chromosomal aberrations are critical for understanding the development, inheritance, and prognosis. While the particular risk factors for developing mutations in critical genes that lead to neuroblastoma have yet to be established, research is focusing on exposures during pregnancy and conception.[17] Despite advances in treatment approaches, the prognosis for high-risk neuroblastoma remains poor, with a significant proportion of patients experiencing disease recurrence or refractory disease.[1]

2.1.1 Cytogenetics

The primary genetic alterations in neuroblastoma include loss or rearrangement of the distal region of chromosome 1's short arm (1p31-term) and amplification of the MYCN gene. These alterations are predominantly observed in advanced-stage tumours, with most neuroblastoma cell lines derived from such tumours.[20]

Chromosome 1 alterations are also observed in other tumours arising from neural crest cells, suggesting the presence of tumour suppressor genes on chromosome 1p. In neuroblastoma, deletions of chromosome 1p consistently occur, resulting in the loss of one copy of chromosome 1p (monosomy). The deletions frequently involve the region from 1p36.1 to 1pter, which harbours at least two potential suppressor genes. Among these, the p73 gene located on 1p36.33 has been identified as a candidate tumour suppressor gene and is deleted in certain neuroblastoma cell lines.[20]

Another significant genetic alteration in neuroblastoma involves the amplification of the MYCN gene situated on chromosome 2p23-23. This amplification is often present in ecDNA and forms homogeneous staining regions (HSRs) in chromosomes. Notably, amplification of the MYCN oncogene is seen in approximately 25% of patients and is associated with the poorest prognosis. [20, 25, 26] While the size of the amplified region varies, the gain of 17q and loss of 1p often correlate with MYCN amplification.[20, 25] Distal 6q-deletion, 19p-deletion and 1q-gain and ATRX, TERT, TP53, or RAS mutations are further genetic changes that have lately been linked to poor outcomes.[27]

2.1.2 SH-EP2 cell line

The SH-EP2 cell line (RRID: CVCL_HF70), also known as Tet2; TET2 and SHEP2, is a human neuroblastoma cell line.[28] It is a far child from the SK-N-SH cell line, which was obtained from the bone marrow metastasis of a four-year-old girl.[29] These cells lack neuritic processes, are substrate-adherent and epithelial-like in shape. The SH-EP cell line is a hyperdiploid human female (XX) cell line with a chromosome count exceeding the typical diploid number of 46. Chromosome 7 is present in three copies instead of the usual three. Next to this, a partial copy neutral loss of heterozygosity at 14q and 22q, as well as a homozygous deletion at 9p21.3 in the region harbouring the genes CDKN2A and CDKN2B, were also found in the SH-EP cell line.[30]

Additionally, the cell line has two sequence variations that have point mutations in the ALK and NRAS genes.[28] The ALK-gene encodes the ALK tyrosine kinase receptor, which is important for the correct functioning and development of the nervous system.[31] The N-RAS, which encodes a Ras protein, which controls intracellular signalling networks by serving as binary molecular switches. Ras proteins are often unregulated in cancer, resulting in increased invasion and metastasis as well as decreased apoptosis.[32]

It has to be emphasized that even stable cell lines undergo changes over time, evolving and acquiring aberrations specific to the cell culture environment rather than reflecting the original tumour. Regular monitoring of cell lines for genetic changes is essential, considering the effects of extended passages in culture.[30] While no single cell line can fully capture the complexity of neuroblastoma, SH-EP2 cells provide a useful model that recapitulates key features of the disease.

2.2 Extrachromosomal DNA

Extrachromosomal DNA (ecDNA) is an emerging area of research in cancer biology that has gathered attention for its role in tumour development and progression.[5, 33, 34] ecDNA is a type of genetic material that exists outside of the chromosomes in the nucleus of a cell. These fragments of DNA have circularised after breaking off from the linear chromosomes. Two types of ecDNA exist: 100 bp to 50 kb elements that are relatively small and located in many different cell types throughout the body but with uncertain functions and 50 kb to 5 Mb bigger oncogenic elements that are only found in cancer cells and contain genes that are known to have an influence on the development of a cell to cancer cell.[35, 33] The presence of ecDNA has been found to play a significant role in tumour heterogeneity, genomic remodelling, and drug resistance.[8] As a result, patients with ecDNA-containing tumours have poorer clinical outcomes than those with other kinds of focal amplification, indicating the functional relevance of ecDNA elements.[36] Between and within tumour types, great diversity exists between focal chromosomal and extrachromosomal amplifications.[37, 38] When the amplification induces increased proliferation and cell survival, these will become more present due to clonal

selection. Studies have shown that a majority of genes amplified at high copy number levels in cancer cells are located on ecDNA rather than within the chromosomes themselves. Furthermore, the presence of ecDNA has been observed in a subset of tumours, specifically in 14% of newly diagnosed and untreated cancers.[36]

2.2.1 Biogenesis

The formation of this ecDNA is a complex process that can occur through various mechanisms, as presented in figure 1. To current knowledge the pathways ecDNA is formed include chromothripsis, mild DNA damage, the episome model, the breakage–fusion–bridge (BFB) cycle, the translocation–deletion–amplification model, and fork stalling and template switching (FoSTeS).[39]

Chromothripsis, also called chromosome shattering, is thought to be generated by a series of DNA damage events triggered by the formation of micronuclei or chromosome bridges during a single cell division. [40, 41, 42] A significant proportion of DNA damage occurs during interphase, when the nuclear envelope of the micronuclei ruptures, exposing enclosed chromosomes to the cytoplasm.[42] Subsequently, during mitosis, cells with micronuclei chromosomes undergo aberrant DNA replication, resulting in a burst of DNA fragments. The ligation of these fragments in random order and orientation generates chromothripsis.[43] In the mild DNA damage model, damage is induced between the two foci of a replication fork. In this process, a free DNA section, which can be end-to-end ligated to form ecDNA, and a homologous repaired DNA strand are formed.[44] The episome model proposes that large, microscopically visible ecDNA is derived from submicroscopic circular episomes, which are a product of drops in the replication bubble caused by DNA replication errors and can gradually expand in cells.[45] The BFB cycle typically begins with a break in a chromosome, forming two separate chromosome fragments.[46] During DNA replication, each fragment is copied, resulting in two pairs of sister chromatids. However, one of the sister chromatids lacks a telomere due to the break.[47] When the cell enters mitosis, the lack of a telomere on one of the sister chromatids triggers a series of events known as the "fusion-bridge" cycle. The sister chromatids without a telomere form a bridge during mitosis, and as the cell divides, the bridge is pulled apart, resulting in the breakage of the bridge. This process can occur repeatedly, leading to a cycle of breakage, fusion, and bridge formation in subsequent cell divisions. Each cycle of breakage and fusion can cause further chromosomal rearrangements and amplifications, which can lead to the formation of abnormal structures, such as dicentric chromosomes or amplified gene sequences.[46] Some of these BFB amplicons may circularize to terminate the cyclic process, resulting in ecDNAs.[8] Gene rearrangements occur at the translocation site in the translocation-deletion-amplification model. Fragments at the translocation breakpoint are amplified, maintained, or deleted, potentially resulting in the development of ecDNA.[48] Finally, the mechanical model of fork stalling and template switching is presented. A DNA lesion causes the replication fork to halt. The lagging strand disengages, anneals to a neighbouring microhomology-rich active replication fork,which initiates DNA synthesis. This procedure can be done repeatedly until the lagging strand returns to the original template and produces ecDNA.[49]

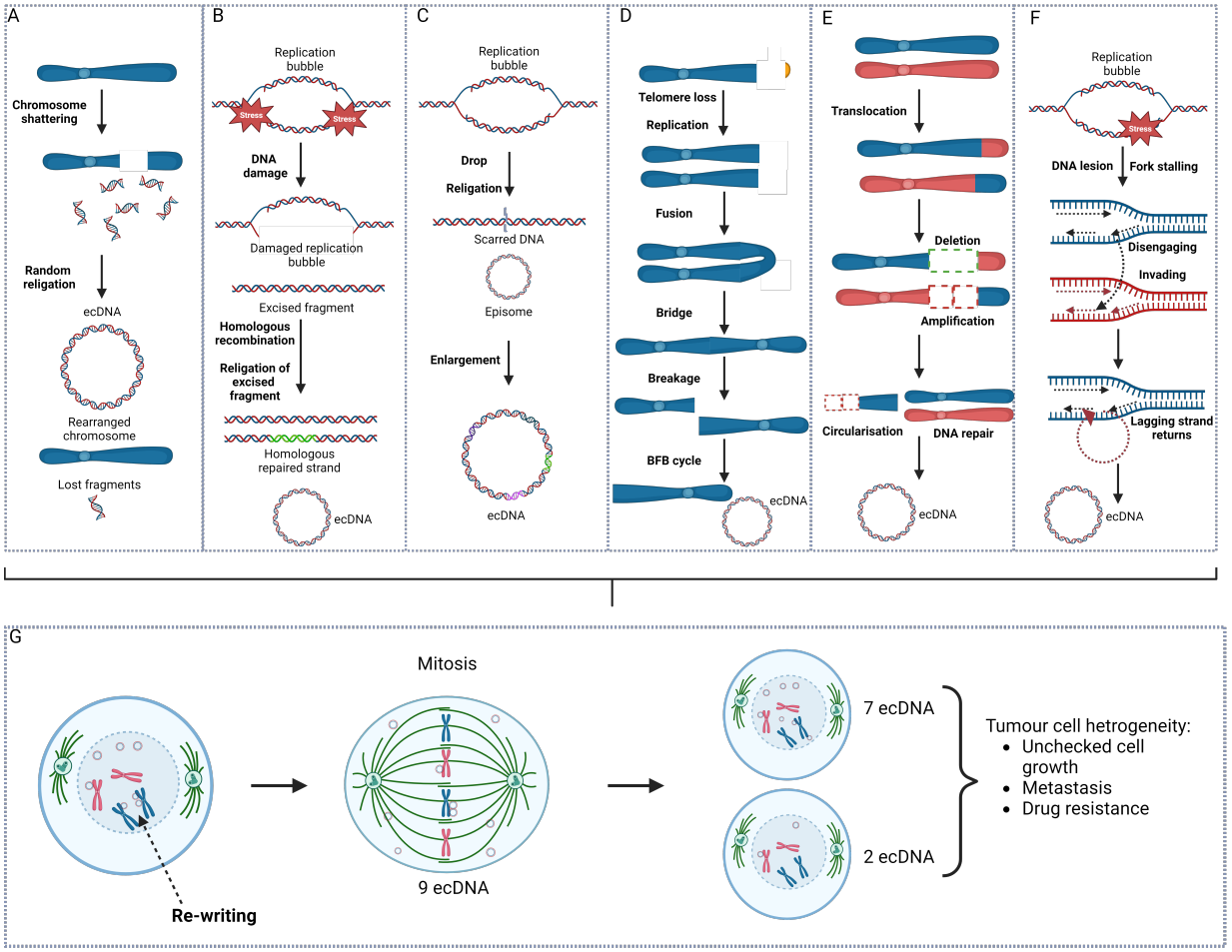

Figure 1: Biogenisis, location and distribution of ecDNA in tumour cells. EcDNA can be produced by a variety of cell cycle events. currently known processes for the formation of ecDNA are (A) chromothripsis, (B) mild DNA damage, (C) the episome model, (D) the breakage-fusion-bridge (BFB) cycle, (E) the translocation-deletion-amplification model, and (F) fork stalling and template switching (FoSTeS). (G) These ecDNA drive tumour heterogeneity via interactions within the nucleus and uneven distribution during mitosis.

2.2.2 Topology

The ecDNA structure is circular, in contrast to chromosomal DNA, which leads to a more open chromatin conformation. This feature allows for gene regulatory interactions that are absent under normal conditions, as presented in figure 2.[50, 51] Firstly, the less compact organisation of the DNA around the nucleosomes makes it more accessible to regulatory proteins.[51] Secondly, ecDNAs often contain functional enhancer elements near target genes resulting from enhancer hijacking, an event in which a somatic structural genomic rearrangement places an enhancer in close proximity to a gene with which it does not ordinarily interact, resulting in high expression levels of that gene.[52] In addition to this, studies have shown that ecDNA molecules cluster together in hubs during both interphase[53, 54] and mitosis[55]. Advanced imaging technologies have allowed the identification of these ecDNA hubs as transcriptional hotspots during interphase.[56] However, not all cell types form these hubs, suggesting the involvement of unknown factors in their formation.[57]

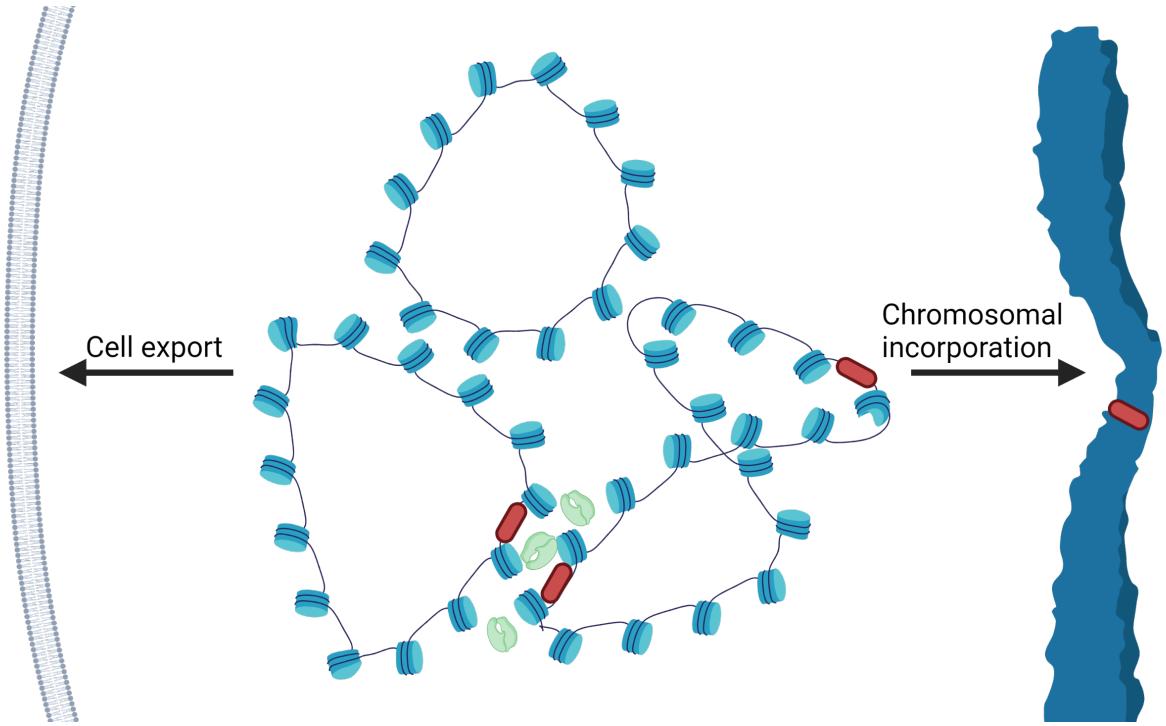

Figure 2: The chromatin structure of circular ecDNAs is open. EcDNAs come together in transcriptional hubs, allowing for trans-regulation between enhancers (red structures). These hubs have been shown to contain RNA Polymerase II (green structures), which is involved in the transcription of the mRNAs. The circularity of ecDNAs provides unique cis-interactions (shown by right ecDNA overlap). EcDNAs may either integrate into chromosomes to form new enhancer interactions or homologous staining regions (HSRs), or they can be exported into the extracellular matrix.

2.2.3 Effect on cell fate

Recent studies have shown that neighbouring enhancer elements, active in the cancer cell type of origin and DNA fragile sites, play a significant role in shaping the borders of ecDNA amplifications.[52, 58] In neuroblastoma, which is commonly associated with extrachromosomal amplification of the MYCN oncogene, two distinct classes of amplicons have been identified. Class I amplicons contain local enhancer elements and have a simple structure with minimal incorporation of distal DNA segments. Class II amplicons lack local enhancer co-amplification but compensate by incorporating DNA segments from distant sites, such as other chromosomes. These distant DNA segments contain lineage-specific enhancer elements and insulators, resulting in complex amplicons with new spatially interacting regulatory regions.[58] These amplicons may be observed on both ecDNA and chromosomes. In the chromosome they can present itself as homologous staining regions (HSR). An HSR is a form of structural alteration in a chromosome, in which a section of a chromosome is amplified or duplicated several times in a specific area of a chromosome. This section contains a particularly high density of a gene or genes that confer a selective advantage to the formation of the tumour. This chromosomal section will get considerably extended as a result of these duplications.[59]

Furthermore, the absence of centromeres leads to a random distribution of ecDNAs during cell division and genes encoded on them are transmitted in a non-mendelian manner.[34] EcDNA can integrate into and exit from chromosomal DNA. The numbers of specific ecDNAs can change in response to treatment. These unique features of ecDNA contribute to the genomic instability and heterogeneity of tumours, which can accelerate their evolution and lead to drug resistance.[7]

3 Extracellular vesicle-associated DNA

3.1 Extracellular vesicles

Extracellular vesicles (EVs) are small, lipid bilayer-enclosed structures that are released by various cell types into the extracellular space. They are involved in intercellular communication and serve as vehicles for transferring biomolecules between cells. EVs play crucial roles in both physiological and pathophysiological processes, including immune responses, tissue repair, tumour formation and cell-to-cell signalling amongst others.[60, 61, 62]

EVs can be classified into subgroups that differ in size, morphology, composition, content and biogenesis. As a result, often extensive isolation and characterisation methods are employed to distinguish these subtypes.[63] However, there is not yet one consensus about the classification of EVs. To establish some guidelines, using the collective knowledge of various researchers, the 'Minimal information for studies of extracellular vesicles' guidelines were published and updated in 2018.[64] The MISEV 2018 guidelines endorse the use of "extracellular vesicle" (EV) as the general term for lipid-bilayer-delimited particles that cannot replicate and lack a functional nucleus released from cells. It is also difficult to assign EVs to specific biogenesis pathways due to the absence of consensus on subtype markers, such as "exosomes" (endosome-origin) and "ectosomes" (plasma membrane-derived).[65] The guidelines recommend using operational terms for EV subtypes based on physical characteristics (size or density), biochemical composition (specific markers), or descriptions of conditions or cell of origin instead of historically burdened terms like exosomes and microvesicles.[64] If these terms are used, they should be clearly defined at the beginning of each publication.[66] In cases where EV identity cannot be confirmed according to the guidelines, terms like "extracellular particle" (EP) may be more appropriate.[64]

In this research, we will classify four main types of EVs according to their size: exosomes, microvesicles, apoptotic bodies and large oncosomes. Exosomes are the smallest type, ranging in size from 30 to 150 nm, and are formed through the inward budding of endosomal membranes. Microvesicles, also known as shedding vesicles or ectosomes, range in size from 100 to 1000 nm and are formed by outward budding or shedding of the plasma membrane. Apoptotic bodies are larger vesicles, typically in the range of 500 to 5000 nm, and are released during programmed cell death (apoptosis). Large oncosomes have a diameter of 1 to 10 μm and are produced and secreted by cancer cells.[67]

3.1.1 Cargo

EVs carry a diverse cargo of bioactive molecules, including proteins, lipids, RNA, and DNA. These molecules can be packaged and protected within the vesicles, allowing them to be delivered intact to recipient cells. The contents of EVs are highly regulated and can reflect the physiological or pathological state of the parent cells.[68, 69] This makes EVs not only a means of intercellular communication but also potential biomarkers for disease diagnosis and prognosis.[69, 70, 71]

Focusing on DNA-associated EVs, these are a subset of EVs that contain DNA molecules inside or on the lipid bilayer.[12] While DNA is known to exist in or on EVs, the mechanism by which the DNA ends up in the vesicle is still not entirely known.[70] Until 2014, the understanding of DNA content in extracellular vesicles (EVs) was limited to single-stranded DNA (ssDNA), mitochondrial DNA (mtDNA), and repetitive transposons.[72, 73] These findings were based on enzymatic methods that allowed researchers to confirm the

presence of DNA in EVs. However, in 2014, significant advancements were made when studies demonstrated the existence of double-stranded DNA (dsDNA) in cancer-derived exosomes.[68, 69]

3.1.2 Biogenesis of exosomes

As mentioned in section 3.1, while size distribution and morphological characteristics might overlap, different types of EVs have different biogenesis and secretion mechanisms. Among the various types of EVs, exosomes have been extensively studied for their biogenesis pathways. The two main pathways involved in exosome formation are the "classic pathway" and the "direct pathway."[65]

The classic pathway of exosome biogenesis is a well-established and extensively studied process. It primarily involves the formation of intraluminal vesicles (ILVs) within multivesicular endosomes (MVEs). These MVEs can then follow two distinct routes: fusion with lysosomes for cargo degradation or fusion with the plasma membrane to release ILVs as exosomes.[74]

Different intracellular sorting pathways exist to direct proteins toward ILVs that are either destined for lysosomal degradation or secretion as exosomes. Proteins sorted for lysosomal degradation are often redundant transmembrane receptors that undergo ubiquitination, a post-translational modification executed by the Endosomal Sorting Complex Required for Transport (ESCRT).[75, 74] Membrane remodelling and protein sorting are processes carried out by ESCRTs. Additionally, the pinching off of ILVs is mediated by the same ESCRTs that mediate budding.[65].

In contrast to the classic pathway, the direct pathway of exosome biogenesis offers a more immediate route. Some cells, such as T cells and erythroleukemia cell lines, release exosomes directly from their plasma membrane. This can occur spontaneously or in response to various stimuli, including the expression of specific viral proteins or cross-linking of surface receptors. However, in some literature, these EVs may be addressed as ectosomes rather than exosomes, while their biogenesis differs quite a bit from that of 'classical' exosomes.[65]

Despite the distinct origin, exosomes formed through the direct pathway share similarities with those from the classic endosomal pathway. They are enriched in classic exosome markers such as TSG101, HSP70, Alix 1, CD9, CD63, CD81, and CD82 and they exhibit similar diameters and densities.[14] However, the extent to which this direct pathway is employed by other cell types or occurs *in vivo*, particularly in biological fluids, remains an area of ongoing investigation.

3.1.3 Extracellular vesicle isolation strategies

Isolation of extracellular vesicles (EVs) has presented a considerable challenge due to the complex nature of body fluids. The isolation process encounters numerous hurdles influenced by various factors, including biological constituents, separation techniques, and limitations of detection methods. The issues surrounding isolation techniques and detection inefficiencies have contributed to the lack of standardised protocols and classification criteria.

Most commonly, the isolation of vesicles involves differential centrifugation, which utilises centrifugal force to separate particles in a solution based on size and density.[64] This

process comprises sequential steps of centrifugation, progressively increasing the force to separate components of different sizes and densities.[13, 76] However, the efficiency of isolating EVs via differential centrifugation is influenced by several factors such as vesicle characteristics, fluid properties, centrifugation parameters, and the type of rotor used. The challenges with differential centrifugation are evident, especially in attempts to isolate specific subpopulations of vesicles. In general, centrifugation steps at 200 to 1500 g are performed to remove cells and debris, centrifugation steps at 10000 to 20000 g are performed to remove larger vesicles and ultracentrifugation (UC) steps at 100000 to 200000 g are performed to remove vesicles with a diameter larger than approximately 100 nm. Despite multiple centrifugation steps, achieving complete separation remains an ongoing challenge due to the heterogeneous nature of vesicles. Therefore, cross-contamination remains a frequent issue.[64]

Density Gradient Centrifugation (DGC) stands as an alternative ultracentrifugation method distinguished by its utilization of a preconstructed density gradient medium within the centrifugation tube. Unlike traditional ultracentrifugation, where the sample is subjected to centrifugation without a predefined gradient, DGC employs mediums such as sucrose and iodixanol to create a stratified density environment.[77] The choice of density gradient media is critical in determining the efficiency and specificity of the separation process. Sucrose has been a longstanding choice, while iodixanol, found in OptiPrep®, presents advantages in terms of its low viscosity and osmolality, contributing to improved vesicle recovery.[13] However, DGC also has its drawbacks. This method is associated with longer cycle durations, a lower yield rate, and the requirement of larger sample volumes compared to traditional UC. The extended processing times may be attributed to the gradual migration of particles through the density gradient. Additionally, the lower yield rate and larger sample volume requirements may pose practical challenges, especially when dealing with limited biological samples.[78, 77]

Filtration methods offer an alternative for vesicle isolation based on differences in size, shape, and deformability. However, challenges such as vesicle deformation, subpopulation binding, and the need for increasing forces with decreasing pore size are encountered. Nanofabricated filtration sieves have shown promise with well-defined pores as small as 100 nm, yet there is a need for further investigation to optimize their use for EV isolation, especially concerning the obtained volume from a given sample.[77]

Other techniques, for instance, micro- and nano-fluidic chips that leverage acoustic, electrophoretic, and electromagnetic technologies to isolate EVs based on their biochemical properties have demonstrated success in isolating exosomes from specific cell types. However, while these techniques are efficient and can be used on small samples, their wide application is limited due to the requirement for extensive optimization and the higher costs compared to differential centrifugation.[77]

The quest for efficient and standardized isolation techniques for extracellular vesicles remains a challenge due to the diverse nature of biological samples and the limitations of available methodologies. In this research, differential centrifugation using a benchtop centrifuge and a dedicated ultracentrifuge will be used while this equipment including protocol is readily available.

3.2 Metabolic DNA labelling with F-ara-EdU

F-ara-EdU, formally known as (2′S)-2′-deoxy-2′-fluoro-5-ethynyluridine, serves as a modified nucleoside analogue of thymidine with widespread application in DNA synthesis studies. It is known to have low cytotoxicity and impact on genome function. [79]

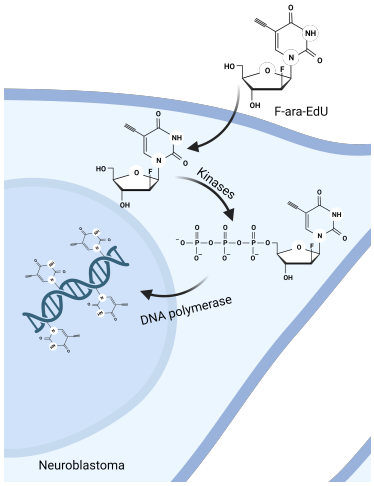

Figure 3: Incorporation of F-ara-Edu into the DNA of a neuroblastoma cell.

The mechanism by which F-ara-EdU functions in DNA synthesis studies involves its incorporation into DNA through phosphorylation by cellular kinases and subsequent integration into replicating DNA strands by DNA polymerases. The process is illustrated in figure 3, showcasing the essential steps leading to the integration of F-ara-EdU into the DNA structure. Once F-ara-EdU is successfully incorporated into DNA, its ethynyl group becomes a target for further modification. For instance, this ethynyl group can be selectively labelled with an azide-containing fluorophore using the copper-catalyzed azide-alkyne cycloaddition (CuAAC) reaction, as depicted in figure 4. This step allows for the visualization and detection of F-ara-EdU-labeled DNA, providing a powerful tool to track and study actively proliferating cells.[79]

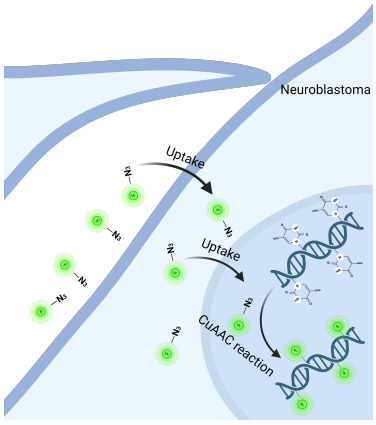

Figure 4: Incorporation of azide-containing fluorophore into the cell nucleus. There it undergoes the CuAAC reaction to 'click' to the synthetic nucleoside labelled DNA.

In the context of studying intercellular DNA transfer via extracellular vesicles (EVs) in culture, F-ara-EdU's dual capability to label DNA and facilitate selective enrichment becomes particularly valuable. By incorporating F-ara-EdU into culture media, it is not only possible to study DNA synthesis dynamics but also discern the origin of EV-DNA and selectively enrich EV-DNA from specific cell populations. This integrated approach enhances the precision and versatility of investigations into the intricate processes of intercellular communication mediated by EVs.

3.2.1 Copper-catalyzed azide-alkyne cycloaddition

The copper-catalyzed azide-alkyne cycloaddition (CuAAC) is a well-studied and widely used 'click reaction' catalysed by a metal ion. It involves the reaction of an organic azide and an alkyne in the presence of a copper catalyst, forming a 1,2,3-triazole as the product.[80, 81] The use of a copper catalyst in water improved on the original reaction proposed by Rolf Huisgen in 1963, which was conducted at high temperatures.[82, 83] This reaction is highly efficient and selective making it an attractive method for a wide range of applications in materials science, medicinal chemistry, and bioconjugation.

Unlike the noncatalyzed version, which can proceed through a concerted or stepwise mechanism depending on the functional groups involved, CuAAC exclusively follows a stepwise process due to the influence of the copper catalyst.[84] A few studies have identified two competing mechanisms for triazole formation in CuAAC. One involves a

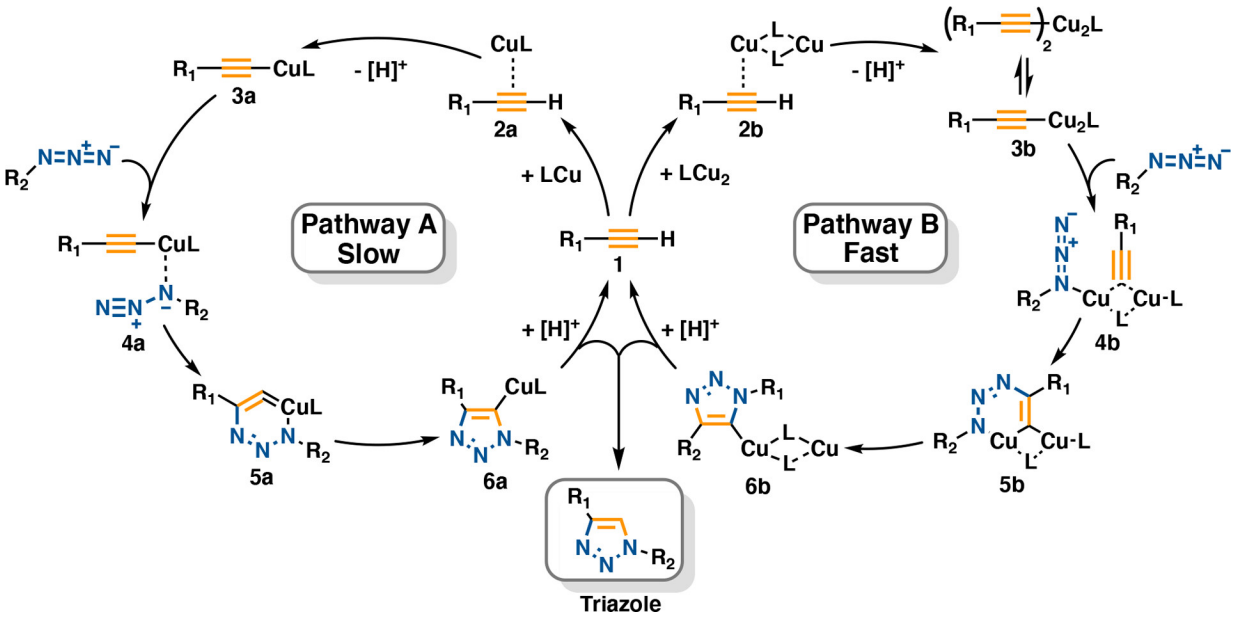

Figure 5: The CuAAC reaction has two competitive pathways: a slow process facilitated by a mononuclear copper species and a more kinetically favoured route through the formation of a dinuclear copper catalyst.[81]

slow process catalyzed by a mononuclear copper species, while the other pathway is more kinetically favoured and promoted by a dinuclear copper catalyst, as presented in figure 5.[80, 84]

The initial step involves the displacement of a ligand from the Cu(I) centre by the organic alkyne, leading to the formation of a π-complex. This step is slightly endothermic in organic solvents, where the solvent environment does not favour the reaction energetically. However, in an aqueous environment, this step becomes exothermic, facilitating the reaction and leading to faster CuAAC reactions in water. The coordination of the organic azide to the copper(I) core or the second copper centre in the dinuclear pathway is crucial. This coordination facilitates the addition of the terminal nitrogen (N-3) of the azide to the carbon (C-2) of the acetylide. This formation creates a Cu(III) metallacycle, an intermediate that significantly reduces the activation barrier for C-N bond formation compared to the uncatalyzed reaction. Following the Cu(III) metallacycle formation, the ring contracts to form the triazolyl-copper derivative, an essential step in the catalytic cycle. The triazolyl-copper derivative undergoes protolysis, leading to the release of the triazole product, thereby completing the catalytic cycle.[81]

Various strategies exist for generating and stabilizing Cu(I) sources for CuAAC reactions. Utilising Cu(I) salts or carbene complexes directly, oxidising or comproportioning Cu(0) sources, and forming the active catalyst from Cu(II) salts by adding reducing agents are the three widely used approaches.[81] In this research, BTTAA (tris-(3-benzyl-4H-1,2,4-triazol-4-yl)amine) is the ligand of choice in the CuAAC reaction. It acts as a chelating ligand that coordinates with the copper ion. This coordination helps to stabilize the copper(I) species, preventing its oxidation to copper(II), which is less effective as a catalyst in the CuAAC reaction. Next to this, it assists in improving the catalytic efficiency of copper in promoting the cycloaddition reaction by binding to the copper centre, it helps in maintaining the catalyst in its active form, enabling the copper to readily interact with both the alkyne and azide components, thus facilitating the formation of the triazole product.[85]

In nucleic acid chemistry research, the in situ generation of Cu(I) catalysts by chemical reduction of Cu(II) salts is a commonly pursued strategy. Aqueous conditions are pre-

ferred due to the high water solubility of most reductants and cupric compounds, making them suitable for nucleotide/oligonucleotide solutions. In this research $CuSO_4$, in combination with sodium-L-ascorbate (Na-L-Asc), a reductant, is used while it has been shown to have high catalytic efficacy. Na-L-Asc is considered a safer option than other reductants, such as TCEP and hydrazine, but its addition to cupric aerobic solutions can lead to reductant oxidation and side reactions. Excessive catalyst loading should be avoided, and anaerobic conditions should be maintained to preserve the integrity of the Cu(I) catalyst and substrates.[81]

4 Experimental procedures

4.1 Cell culture

SHEP-2 cells were cultured in a T25 culture flask at 37°C, 5% CO_2, until experimental use. The cells were maintained in complete culture medium [Dulbecco's Modified Eagle Medium (DMEM)(Capricorn, Ebsdorfergrund Germany) supplemented with 10% fetal bovine serum (FBS)(Sigma-Aldrich, Taufkirchen, Germany), 2mM L-glutamine (Lonza, Basel, Switzerland), 1% MEM non-essential amino acids (Gibco, Karlsruhe, Germany), 1% penicillin-streptomycin (pen/strep)(Lonza) and 1 mM sodium pyruvate (Gibco)]. The cell line was sub-cultured every 3-4 days. Cells were washed with PBS (Sigma-Aldrich) and detached using 0.25% Trypsin-EDTA. A new T25 culture flask was seeded at 5000 cells/cm^2, by adding fresh culture medium to a part of cell suspension.

4.2 Metaphase chromosome spreads

Coverslips with a diameter of 20 mm were sterilized with 70% ethanol and placed in a well of a 12-well plate. These were washed twice with MilliQ and once with PBS. Coverslips were kept on PBS until cell seeding. SH-EP2s were seeded at 5000 cells/cm^2. 12-well plates were incubated at 37°C and 5% CO_2 for 72h for optimal cell adherence. Samples were treated with KaryoMAX Colcemid (Gibco) at 100 ng/ml in DMEM supplemented with 1 mM sodium pyruvate for 2 h to concentrate cells in metaphase. Coverslips with cells were incubated in pre-warmed 75 mM KCl for 30 minutes at 37 °C. Cells were then fixed with Carnoy's fixative [methanol and acetic acid (3:1)] for 15 min. Cells are washed with 1X PBS and stained with 4,6-Diamidino-2-phenylindole (DAPI) (100 ng/ml) for 15 minutes. Samples were washed three times with 1X PBS and coverslips were mounted on microscopy slides using Dako mounting medium.

4.3 Fluorescence in situ hybridisation

Fixed samples on coverslips were equilibrated in 10% formamide in 2× SSC buffer for 2 min. They were then dehydrated in ascending ethanol concentrations of 70, 85 and 100% for approximately 2 min each. Coverslips were airdryed. MYCN fish probe was diluted in hybridization buffer (MYCN-20-OR, Empire Genomics) as recommended by the manufacturer. 8.26 μL of probe solution was dropped on a microscopy slide and closed by the fixed samples on the coverslip. Coverslips were closed off with rubber cement to minimize probe evaporation. Samples were denatured at 73 °C for 2 min and then hybridised at 37 °C overnight in a humid and dark chamber. Samples were then washed with 0.3% igepal in 0.4× SSC at 73°C and then in 0.1% in 2× SSC at RT (all washes lasting approximately 2 min). DAPI (100 ng/ml) was applied to samples for 15 min. Samples were washed three times with 1X PBS and coverslips were mounted using Dako mounting medium.

4.4 Microscopy

Conventional fluorescence microscopy was performed using a Nikon Eclipse E400 microscope equipped with a 100X oil immersion objective; images were acquired with a Hamamatsu Orca-flash 4.0lt plus camera. Confocal microscopy was performed using a Zeiss LSM880 confocal microscope equipped with a Zeiss C-Apochromat 63x/1.20 W Corr M27 objective. Image processing is performed in Fiji (Fiji Is Just ImageJ), an open-source image processing package based on ImageJ2.

4.5 EV-associated DNA quantification

4.5.1 EV isolation

SH-EP2 cells were seeded in T182.5 culture flasks at 5000 cells/cm^2 in complete culture medium and incubated for 72h. Cells were washed with PBS and supplemented with DMEM-HA culture medium supplemented with 1 mM sodium pyruvate. Flasks were incubated at 37 °C for 48h for EV generation. EVs were harvested from the supernatant of the culture medium using centrifugal separation. First, centrifugation steps (300g, 10 min at RT and 2000g, 20 min at 4 °C) were performed. Additionally, EVs were pelleted using ultracentrifugation (110000g, 2.25h at 4 °C) using a Beckman Coulter ultracentrifuge equipped with a MLA-50 fixed-angle aluminium rotor. The supernatant was decanted and the pellet was resuspended in 200 μL Tris-HCl buffer [(10mM Tris-HCl, 2.5 mM $MgCl_2$, 0.5 mM $CaCl_2$), pH 7.4] or 1X PBS (pH 7.4) supplemented with 2.5 mM $MgCl_2$, 0.5 mM $CaCl_2$.

4.5.2 DNase treatment

EV samples from two different culture flasks were combined, homogenised and split again, to create similar starting materials for DNA quantification with and without treatment with desoxyribonuclease. Half of the samples were treated with 100 μg/mL DNase I (Roche, Basel, Switzerland) for 30 min at 37 °C to eliminate all external DNA. The DNase I was inactivated by the addition of Ethylenediaminetetraacetic disodium salt (EDTA-Na_2) (Sigma-Aldrich) to a final concentration of 5 mM and a 10 min heat inactivation step at 75 °C.

4.5.3 DNA isolation and quantification

DNA was isolated from enriched EVs produced by SHEP-2 cells using a QIAamp DNA Mini Kit (Qiagen, Hilden, Germany) and a phenol-chloroform extraction method. The implementation of the DNA isolation kit was according to the manufacturer's protocol. For the phenol-chloroform extraction, phenol/chloroform/isoamyl alcohol (PCI) mixture (25:24:1) (Sigma-Aldrich) was added to the sample. DNA will stay in the aqueous phase, while lipids will solubilize in the organic phase and proteins will gather at the interphase. The aqueous phase was isolated and a back extraction, using chloroform (Sigma-Aldrich) was done to further purify the DNA sample. Lastly, ethanol precipitation is performed using 70% etOH, 20 μg glycogen (Thermo Scientific Chemicals, Waltham, Massachusetts, USA) and 0.75 M ammonium acetate (Sigma-Aldrich). The DNA pellet was washed thoroughly with 70% ethanol and resuspended in 200 μL Tris-HCl. Samples were analysed for DNA quantity with a Qubit dsDNA HS Assay kit (Invitrogen, Waltham, Massachusetts, USA) according to a protocol supplied by the manufacturer. Resuspended DNA was separated on 1% agarose gel (Sigma-Aldrich). Gel was run for 60 min at 90V using TAE buffer [40mM Trizma base (Sigma-Aldrich), 1mM EDTA (Sigma-Aldrich), 1.14 % glacial acetic acid (Carl Roth, Karlsruhe, Germany)].

4.6 Bioorthogonal metabolic DNA labeling

Coverslips with a diameter of 20 mm were sterilised with 70% ethanol and placed in a well of a 12-well plate. coverslips were washed twice with MilliQ and once with PBS. Coverslips were kept on PBS until cell seeding. SH-EP2s were seeded at 3300 cells/cm^2. 12-well plates were incubated at 37°C and 5% CO_2 for 48h for cell adherence. Consecutively, the medium is changed to DMEM-HA supplemented with 10% FBS, 1 mM sodium pyruvate and 100 μ M (2′S)-2′-deoxy-2′-fluoro-5-ethynyluridine (F-ara-EdU) (Click Chemistry Tools, Scottsdale, Arizona, USA) and incubated for 48h. To fix the sample, coverslips

were washed with pre-warmed Hank's Balanced Salt Solution (HBSS) (Gibco) and submerged in 4% PFA for 15 min. After fixation the samples are washed three times with PBS, permeabilized in 0.2% Triton X-100 for 20 min, denatured in 2M hydrochloric acid and neutralized with 0.1M borax for 10 min. After a thorough wash with PBS, 1mL of freshly prepared CuAAC staining mix (5μM AlexaFluor 488 azide (Jena Bioscience, Dortmund, Germany), 50 μM $CuSO_4$, 300 μM BTTAA, and 2.5 mM sodium-L-ascorbate) is added and incubated for 1 h at RT in the dark. Samples were washed with PBS and counterstained with 4,6-Diamidino-2-phenylindole (DAPI) (100 ng/ml) for 15 min. Samples were washed three times with 1X PBS and coverslips were mounted using Dako mounting medium. Evaluation of staining was performed by fluorescence microscopy as presented in section 4.4.

4.7 Detection of DNA transfer

4.7.1 Detection of bioorthogonal metabolically labelled DNA in gel electrophoresis

SH-EP2 cells were cultured as presented in section 4.5, either with or without the addition of 100μM F-ara-EdU. Cells were washed with PBS and supplemented with DMEM-HA culture medium supplemented with 1 mM sodium pyruvate and 100μM F-ara-EdU. Flasks were incubated at 37 °C for 48h for EV generation. EVs were isolated following the centrifugation, ultracentrifugation, DNase I treatment and DNA isolation steps as previously stated in section 4.5. To the sample, a 20X CuAAC staining mix [100μM Cy5 azide (Sigma-Aldrich), 1 mM $CuSO_4$, 6 mM BTTAA, and 50 mM sodium-L-ascorbate] was added 1:20 and incubated for 1h in the dark. 30μL out of 200μL resuspended DNA was separated on 0.7% agarose gel. Gel was run for 30 min at 90V using TAE buffer.

4.7.2 Detection of bioorthogonal metabolically labelled DNA in cell culture

SH-EP2 cells were cultured as presented in section 4.5. Cells were washed with PBS and supplemented with DMEM-HA culture medium supplemented with 1 mM sodium pyruvate and 75μM F-ara-EdU. EVs were isolated as presented in section 3.1.3 and resuspended 1X PBS (pH 7.4) supplemented with 2.5 mM $MgCl_2$, 0.5 mM $CaCl_2$. This EV suspension derived from one T182.5 flask was added to 6 mL DMEM-HA supplemented with 10% FBS and 1 mM sodium pyruvate. In a 12-wells plate, SHEP-2 and LNCaP cells were seeded on coverslips at 10000 and 25000 cells/cm^2 respectively and incubated for 2 days. After this, the cells were washed once with PBS and supplemented with a culture medium containing EVs. Plates were incubated for 1, 3 and 24h. Cells were gently washed with pre-warmed (37°C) HBSS, fixed with 4% PFA for 15 min and washed three times with PBS. AF488-azide was linked to the F-ara-Edu containing DNA as presented in section 4.6. After this, the samples were stained with Memglow560 (Biozol, Hamburg, Germany) for 10 min and DAPI for 15 min, each with a PBS washing step in between. Samples were washed three times with 1X PBS and coverslips were mounted using Dako mounting medium. Detection of fluorophores was performed with a confocal microscope as presented in section 4.4.

5 Results

5.1 Visualization of ecDNA

5.1.1 Metaphase chromosome imaging

The first objective was to observe ecDNA fragments within the nucleus of the SHEP-2 cells. While this was not known from the literature, slides with cell cultures concentrated in metaphase were produced and evaluated under a fluorescence microscope. As presented in figure 6, treatment with 100 ng/mL KaryoMAX colcemid for 24h yielded a higher amount of cells in metaphase and also lower cell density.

To optimize the metaphase procedure a variety of incubation times were tested: 2, 4, 6, 16, 24, 48 and 72h. In all cell preparations with a higher incubation time than 24h, no adherent cells were left. 2, 4, 6 and 16h of incubation times showed, upon visual inspection, no major differences in the amount of cells in metaphase. Overall, higher-density areas had fewer metaphases and lower-density areas had more. Therefore, 2h of incubation with KaryoMAX colcemid was deemed sufficient.

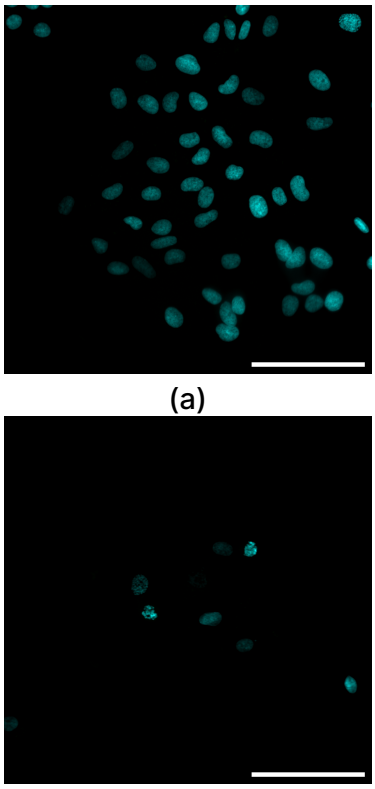

(a)

(b)

Figure 6: **Increase in metaphases in cell preparation when subjecting cells to KaryoMAX Colecemid.** Shown are cell preparations stained with DAPI, (a) untreated and (b) treated for 24h with KaryoMAX Colcemid. Scalebar is 100 μm

However metaphase-containing cell preparations could be made, DNA elements within the nucleus could not yet be distinguished from each other. The nucleus was still too condensed and chromosomal structures were overlapping. Therefore, before cell fixation, a 0.75mM potassium chloride solution was added to the cells. However, the exposure time of cells to this solution will influence their size increase. Too long incubation could lead to cell rupture and lost DNA fragments. Therefore different incubation times with KCl were tested. Cell membrane integrity was evaluated after fluorescently labelling the membrane with Memglow488.

In all KCl parameters, areas could be found where all cell membranes were still intact. In figure 7, a view of each condition is given. Cell swelling and busting were mainly dependent on the local cell density. Cells in less confluent areas seemed to be more prone to bursting. However, longer incubation times with KCl decreased the total amount of cells present on the coverslip, while all cells in low confluence areas burst and were washed away. In this case, while 30 min swelled the cells without excessive loss of cells on the coverslip, this was the chosen method.

After all optimisation, ecDNA was tried to distinguish from chromosomes in the metaphase spreads of SHEP-2 cells. Pictures of representative metaphase spreads are shown in figure 8. The primary challenge in identifying ecDNA lies in the overlapping chromosomal fragments evident in the metaphase spreads, as illustrated in Figure 8. Despite all optimisation performed, this complexity rendered it exceedingly difficult to observe individual

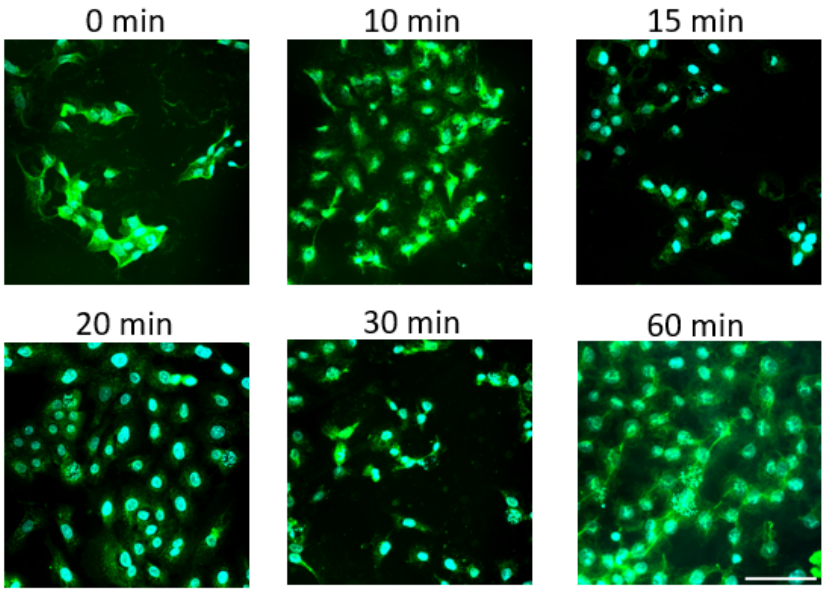

Figure 7: **Membrane integrity and metaphase spread evaluation.** An overview of metaphase spreads of SHEP-2 cell cultures after a variety of incubation times with 75mM KCl (shown in image). DNA is stained with DAPI (cyan) and the membrane is stained with the membrane probe Memglow488 (green). Scalebar is 100 μm.

chromosomes distinctly. Figure 9, shows the only image of the chromosomes in which they are not overlapping. This image indicates that the depicted cell contains 47 chromosomes and does not possess any ecDNA. However, based on the metaphase spreads in Figure 8, it cannot be conclusively asserted that this total absence applies universally to other cells.

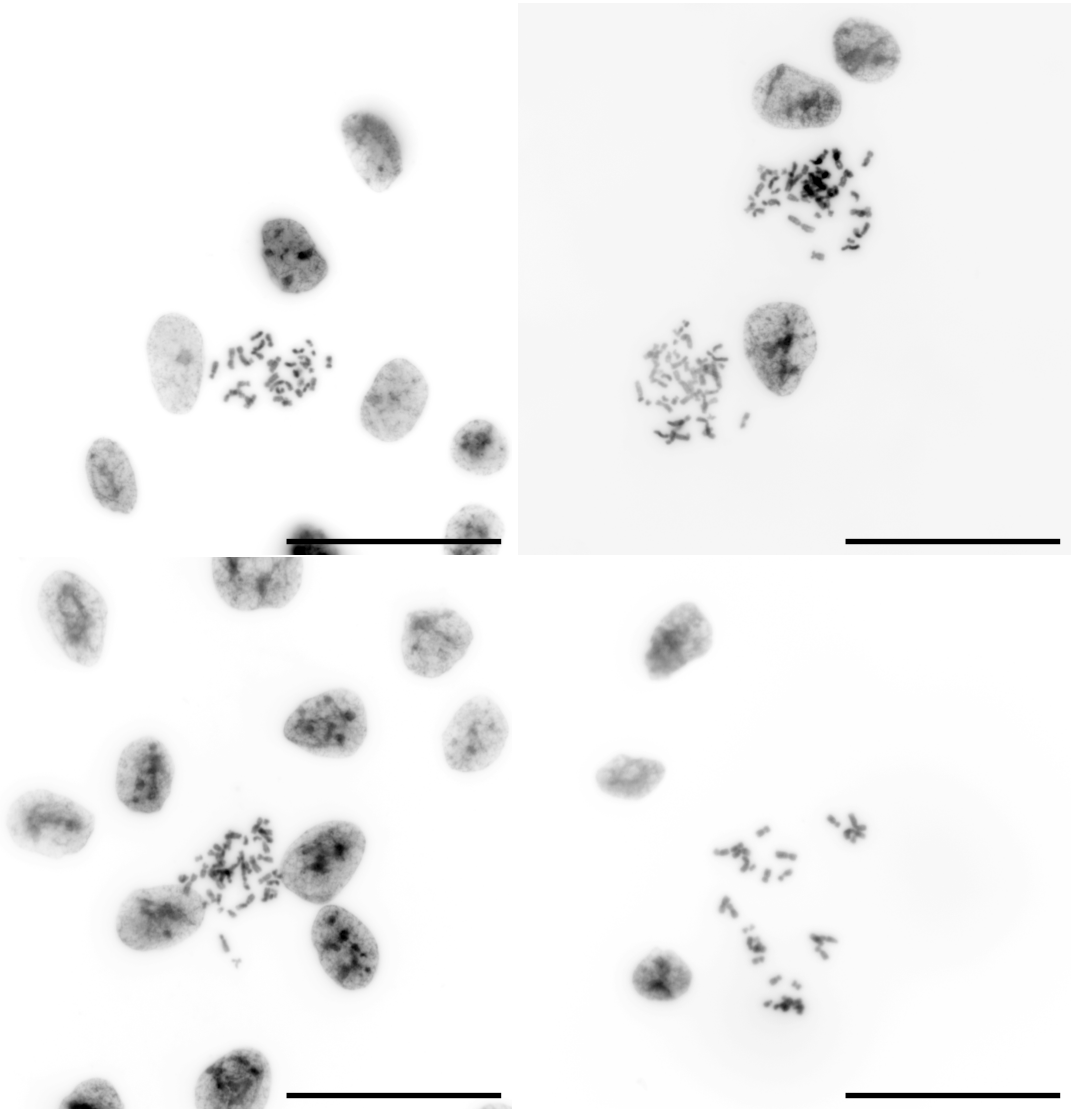

Figure 8: **Four chromosome spreads of SH-EP2 cells.** Obtaining high-quality metaphase spreads proved challenging due to the intricate nature of overlapping DNA structures, making the quantification of fragments not possible. Scalebar is 50 μm

5.1.2 Fluorescent in situ hybridisation

If it is known what gene is often amplified on the ecDNA of a cell line, we can target that gene using fluorescence in situ hybridisation. As discussed in section 2.2.3, neuroblastoma is commonly associated with extrachromosomal amplification of the MYCN oncogene. By linking a fluorophore to this gene we can see if this gene is amplified in the SHEP-2 cell line and if this amplification occurs on many DNA fragments, these might be ecDNA. Samples were prepared according to the protocol presented in section 4.3. However, after implementing this protocol two times with different fixation protocols, the one using Carnoy's fixative and the other using 4% PFA, no clear FISH signal could be observed using the confocal microscopy. To rule out that, this specific cell line does not contain the MYCN gene, the procedure was performed on SHEP-2 and LNCaP, human prostate adenocarcinoma, cells in parallel. Here the same results were obtained for both cell lines: the probe could be detected.

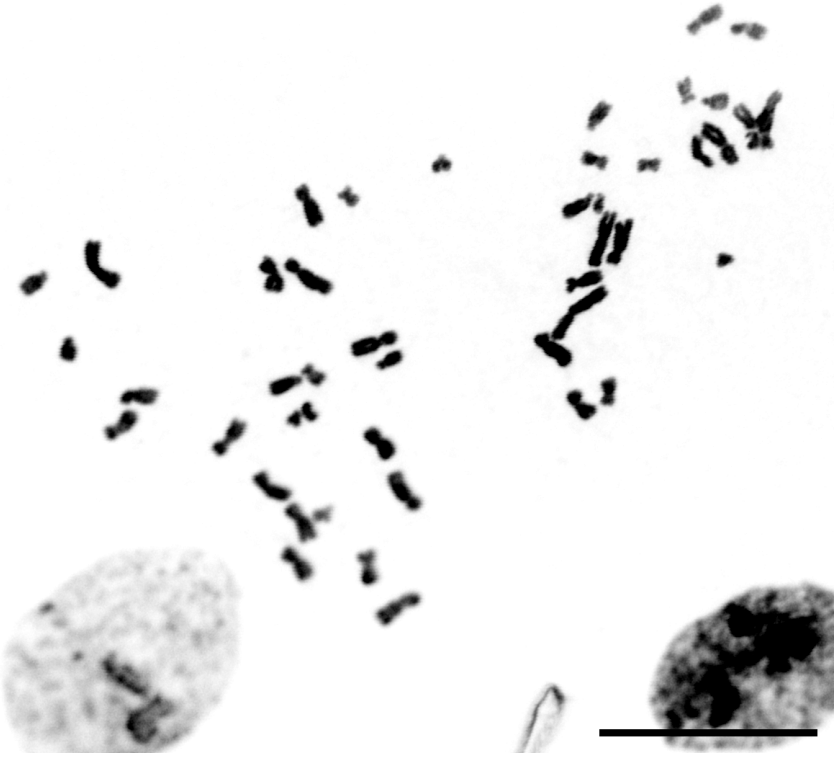

Figure 9: **A metaphase spread of a SHEP-2 cell in which all chromosomal structures can be seen without overlapping.** The chromosome count in this cell is 47 and deviates from the diploid chromosome number(46). Scalebar is 20 μm.

5.2 Bioorthogonal metabolic labelling

From the literature, there is suggestive evidence pointing towards ecDNA transfer through extracellular vesicles (EVs), making them a potentially intriguing target for further investigation. Detecting and following the DNA contents from these EVs could provide valuable insights into ecDNA quantity and the occurrence of this transfer phenomenon within the SHEP-2 cell culture.

Through the application of a bioorthogonal metabolic labelling approach utilizing F-ara-EdU, we can identify or separate the nuclear DNA synthesized by the target cell. This proves advantageous in the search for this particular DNA within EVs. In our pursuit of effective cellular DNA labelling to facilitate subsequent localization studies, we executed a sequence of experiments to evaluate the efficacy of the bioorthogonal metabolic CuAAC click-labelling technique in adherent cell cultures. The primary objective involved the initial labelling of cell nuclei using the CuAAC reaction in conjunction with metabolic labelling. Subsequently, the refined parameters derived from these experiments will be employed in labelling DNA extracted from EV fractions.

To achieve this, we systematically explored the influence of F-ara-EdU concentrations and incubation times on cellular DNA labelling. Coverslip-adherent SH-EP2 cells were subjected to 10, 100 and 200 μM F-ara-EdU and incubated for 48 hours. As discussed in section 3.2, this synthetic nucleoside analogue of thymidine will be incorporated into the DNA by the cell. Subsequent labelling of the analogue with a fluorophore, in this case AF488, visualises this DNA under the fluorescence microscope. The staining was evaluated through fluorescence microscopy, as detailed in figure 10, and yielded sufficient labelling efficiency for 100 and 200 μM. Cells cultured on coverslips were very fragile, so due to harsh washing fewer cells were present on some coverslips. While it was ex-

pected that higher concentrations of F-ara-EdU would contribute to poorer adhesion to the coverglass, 100 μM was chosen for the CuAAC click-labelling technique utilized in the EV-DNA labelling experiments presented in section 5.4.

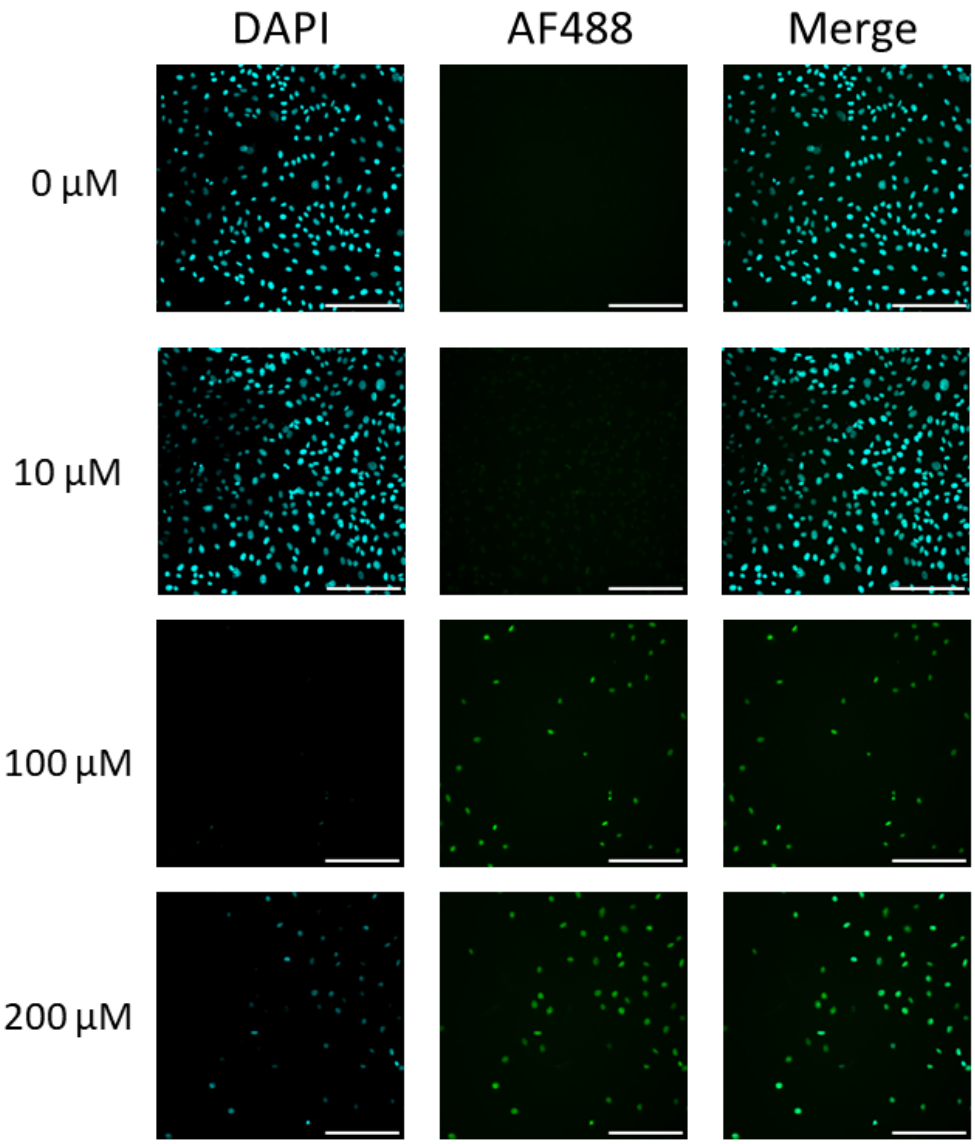

Figure 10: **Effective bioorthogonal metabolic labeling of SHEP-2 cells using F-ara-EdU**. SHEP-2 cells were seeded at 3300 cells/cm^2 and were cultured for 4 days on glass coverslips in a 12-well plate to adhere and reach sufficient confluence. After 2 days the cells received 0, 10, 100 or 200 μM F-ara-Edu. DAPI (cyan), AF488 (green) signal and merged picture obtained after CuAAC labelling of F-ara-EdU with AF488-azide. Scalebar is 200 μm

.

5.3 EV-DNA quantification

The goal was to determine whether EVs carry DNA and whether it resides inside, outside or in both. The strategy involves obtaining EV fractions from cultured cells through a series of centrifugation steps, including ultracentrifugation. The resulting pellets are initially resuspended in Tris-HCl buffer. To investigate whether EVs carry DNA and to determine its location (inside, outside, or both compartments), the experiment employs an enzymatic digestion of non-enclosed DNA in some parameters. To mitigate potential DNA fragmentation caused by conventional column-based DNA purification methods, the approach integrates phenol-chloroform extraction alongside the column purification process.

To discriminate and quantify internal and total DNA from extracellular vesicles (EVs), the two purification methods were employed either with or without enzymatic DNA digestion to eliminate non-enclosed DNA. With column purification and no DNase treatment, the extracted DNA was measured at 13.22 $\pm$ 3.71 ng, corresponding to 1.13 $\pm$ 0.34 ng DNA per 10^6 producer cells (n = 3). Utilizing a phenol-chloroform extraction protocol without DNase treatment, we obtained 6.44 $\pm$ 0.37 ng DNA, with 0.85 $\pm$ 0.09 ng DNA per 10^6 producer cells (n = 3), as illustrated in figure 11a, suggesting the presence of DNA both inside and outside the EVs. Negative control (culture medium), gave a DNA quantity below the detection limit (<100 pg). Positive control (10^6 cells), gave a DNA quantity of 565 $\pm$ 21.0 ng DNA. Agarose gel results (figure 11b) displayed a smear between 1 and 10 kb for non-treated EV-DNA fractions, strengthening the observation of the presence of DNA both inside and outside the EV. Quantities obtained from column extraction revealed approximately 6 to 20 times more DNA in total from the EV compared only to the inside, while phenol-chloroform extraction indicated a ratio of 6 to 10.

In a subsequent experiment, the EV pellet obtained post-ultracentrifugation underwent resuspension in an isotonic 1X PBS solution supplemented with $MgCl_2$ and $CaCl_2$. This modification aimed to counteract any potential adverse effects on EVs, such as swelling or bursting, that could arise from the hypo-osmotic conditions of the initial Tris-HCl buffer. By conducting this supplementary experiment, we not only sought to confirm the DNA quantity in the EV fractions under these altered conditions.

While the previous phenol-chloroform extraction did not yield significantly different DNA yields and induced less DNA shearing according to literature concerning column extraction, it emerged as the preferred method for DNA extraction from EV fractions resuspended in PBS. This approach resulted in 21.69 $\pm$ 0.01 ng DNA without DNase treatment and 4.96 $\pm$ 0.27 ng DNA per 10^6 producer cells with DNase treatment (n=2), as depicted in figure 12a. Negative control (culture medium), gave a DNA quantity below the detection limit (<100 pg). Positive control (10^6 cells), gave a DNA quantity of 733.2 $\pm$ 157.8 ng DNA.

Notably, the total/internal EV-DNA quantity ratio decreased to approximately 4.4 when EVs were resuspended in PBS, compared to the Tris-HCl buffer. This shift suggests that a fraction of EVs lysed in the hypo-osmotic Tris-HCl buffer, rendering some internal DNA susceptible to DNase. Resuspending EVs in PBS also increased the overall isolated DNA quantity.

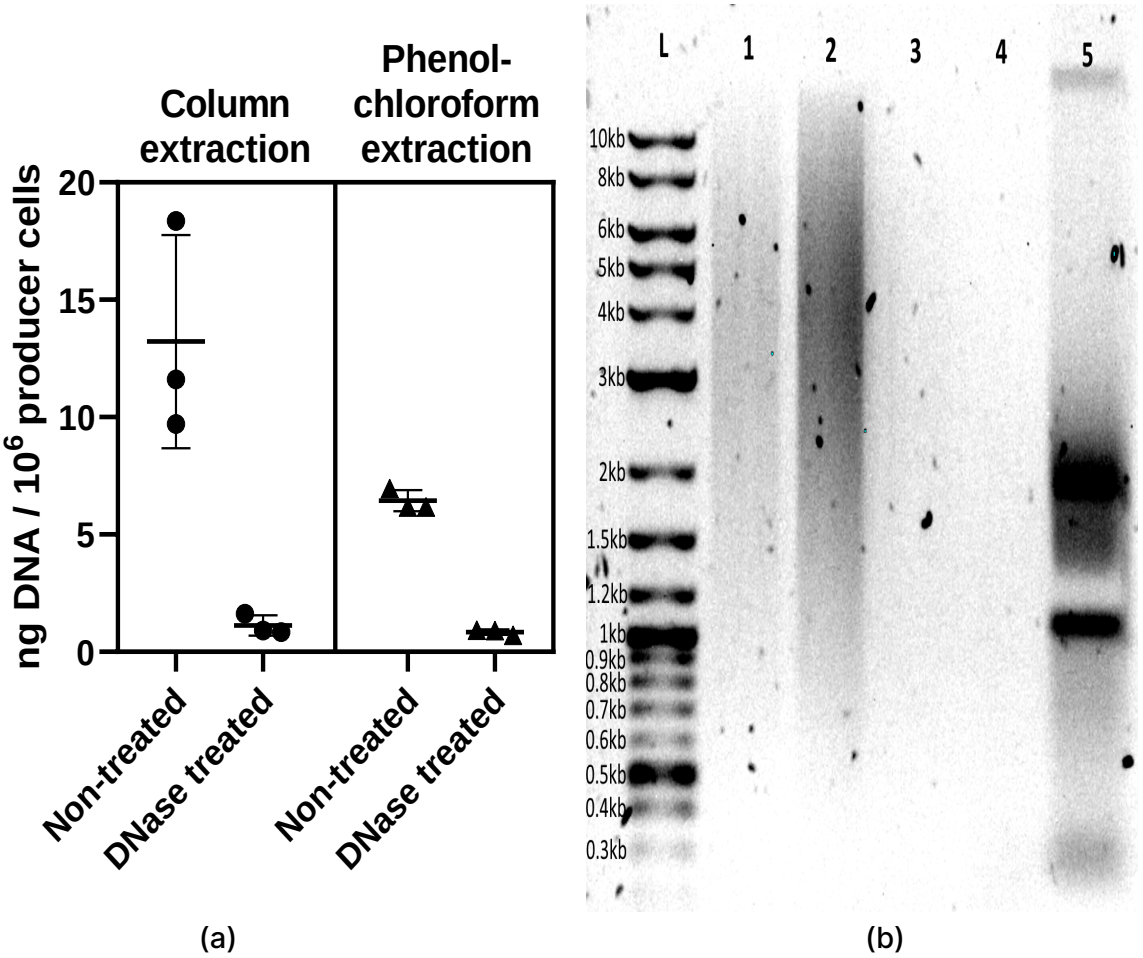

(a) (b)

Figure 11: **Quantification of DNA isolated from in Tris-HCl buffer resuspended EV pellet obtained by ultracentrifugation.** (a) DNA quantities obtained from the EV pellets normalized to million producer cells for two extraction methods without and with treatment with DNase I (n=3). Culture medium was taken as negative control and genomic DNA of one million cells was taken as positive control. To determine that two conditions are significantly different, a two-sided t-test is performed. For both extraction methods the non-treated fraction was significantly different from the treated fraction ($P<0.05$). (b) To substantiate the results of DNA quantification 30 μL of the sample was loaded on a gel. (L) DNA ladder, (1) Phenol-chloroform extraction, (2) Column extraction, (3) Phenol-chloroform extraction (DNase treated), (4) Column extraction (DNase treated), (5) genomic DNA from 10^6 cells.

5.4 Detection of DNA transfer through EVs

5.4.1 Detection of labelled EV-DNA in gelelectrophoresis

To identify horizontal DNA transfer by EVs, cells were exposed to a culture medium containing 100 μM F-ara-EdU. The cell incorporates this synthetic thymidine analogue into its DNA. As shown in figure 5, the nucleoside is sufficiently built into the DNA for visualisation. However, it is not known if these cells package the newly synthesised DNA in EVs within 2 days. Therefore an additional parameter, 5 days of incubation with 100 μM F-ara-Edu is included. Subsequently, the analogue is labelled with a fluorophore, specifically Cy5-azide in this case, allowing the visualization of the DNA under a fluorescence microscope. Successful visualization of the fluorophore-tagged DNA in the EV fraction demonstrates the transfer of nuclear DNA by EVs. To achieve tagging, a 20X CuAAC staining mix was introduced to the EV samples at a 1:20 ratio and incubated for 1 hour in the dark. Subse-

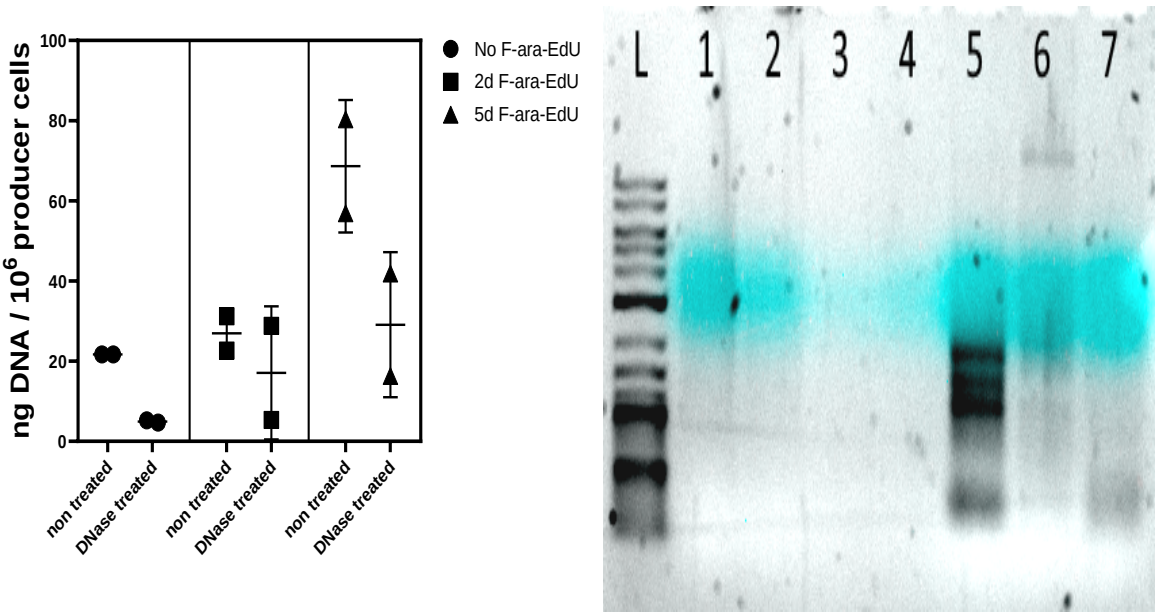

(a) (b)

Figure 12: **Quantification of F-ara-EdU labelled DNA isolated from in PBS buffer resuspended EV pellet obtained by ultracentrifugation.** (a) DNA quantities obtained from SHEP-2 cells including incubation with 100 μM F-ara-Edu for 0, 2 and 5 days. (b) Gel electrophoresis of F-ara-EdU labelled DNA. (L) 0.1kb to 10kb DNA ladder, (1) 2d F-ara-EdU, (2) 5d F-ara-EdU, (3) 2d F-ara-EdU (DNase treated, DT), (4) 5d F-ara-EdU (DT), (5) 5d F-ara-EdU 10^6 cells, No F-ara-EdU 10^6 cells, No F-ara-EdU 10^6 cells (DT). The blue band is unbound Cy5-azide. No DNA-bound fluorophore could be detected after letting the unbound fluorophore diffuse out of the gel.

quently, 30 μL of resuspended DNA was separated on a 0.7% agarose gel. Unexpectedly, the Cy5 azide did not exhibit binding affinity to the DNA. Gel electrophoresis and visualization showed that the Cy5 fluorescence signal did co-localize with the DNA bands in each sample at the same height. Even for the samples that were not treated with F-ara-EdU. This suggests that the anticipated click reaction between the azide group of Cy5-azide and the ethynyl group of the DNA, characteristic of the CuAAC reaction, did not occur as anticipated, as presented in figure 12b.

Upon washing the gel to remove unbound or non-reacted components, the DNA bands remained visible, indicating the presence of DNA fragments. Intriguingly, the Cy5 fluorescence signal disappeared after washing, reinforcing the notion that the expected binding between Cy5-azide and DNA did not take place. This outcome prompts a reevaluation of the CuAAC click-labeling technique with Cy5-azide for detecting horizontal DNA transfer through EVs.

Additionally, an interesting observation was made regarding the duration of F-ara-Edu incubation. Prolonged exposure led to an increase in isolated DNA quantity per million cells, as presented in figure 12a, suggesting that a substantial portion of the isolated DNA may originate from apoptotic sources.

5.4.2 Detection of labelled EV-DNA in cell culture

The goal of this experiment was to investigate whether F-ara-EdU labelled DNA in EV fractions would be detectable using fluorescence microscopy when supplemented to culture medium different cells. SHEP-2 and LNCaP cells were cultured and supplemented with EVs isolated from T182.5 flasks with F-ara-Edu labelled SHEP-2 cells. Following incubation with an EV-containing medium, cells were fixed, and the DNA was CuAAC labelled with AF488-azide. Memglow560 staining was intended to identify labelled DNA's localization as it would mark cell borders, and DAPI staining facilitated visualization of the nucleus.

Despite the planned procedures, at first, the experiment encountered difficulties in distinguishing between labelled DNA and lipid clusters in fluorescence microscopy due to spectral overlap in the emission spectra of Memglow560 and AlexaFluor488, as presented in figure 13a. This challenge, especially evident when determining the look-up table in the Fiji software, hindered accurate result interpretation. With the confocal microscopy, it was possible to distinguish the two fluorophores and construct 3D images to evaluate the image in multiple dimensions, as presented in figure 13b. However, no signal for AF488 could be found in all taken images and incubation times. It was not known if the EV fraction would contain F-ara-EdU labelled DNA, which further complicated the search. Furthermore, most of the cell membranes were ruptured, which would make establishing the location of the labelled DNA difficult.

Regrettably, the technical challenges encountered in this experiment prevented the derivation of meaningful results regarding the interaction between EVs and cellular DNA. However, the conceptual framework of the experiment, designed to investigate ecDNA transfer between cells, remains promising. Future experiments are necessary to explore the potential of ecDNA tracking and horizontal DNA transfer mediated by EVs in cellular models.

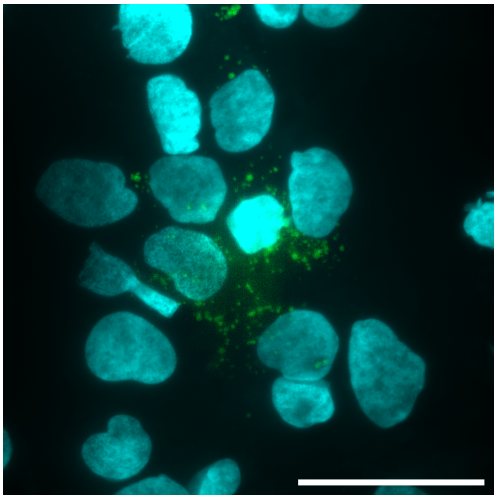

(a)

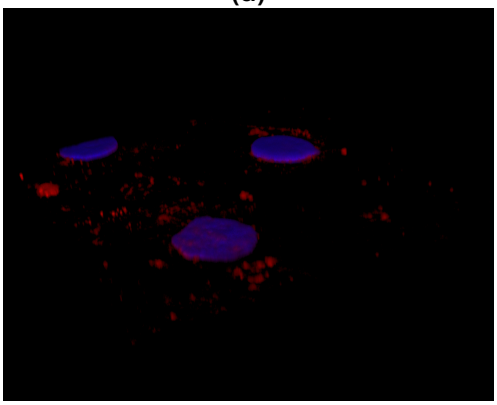

(b)

Figure 13: **Transfered metabolically labelled DNA was not observed with (a) fluorescence microscopy and (b) confocal microscopy.** (a) Image of SHEP-2 cells incubated for 1h with EV-containing medium. Due to spectral bleed-over lipids stained with Memglow560 (red) ended up in the fluorescence channel used for the detection of AF488 (green) labelled DNA. Scalebar is 50 μm (b) Constructed 3D image of LNCaP cells incubated for 1h with EV-containing medium using confocal microscopy. Lipids are stained with Memglow560 (red) and nuclei are stained with DAPI (blue). No AF488 (green) could be detected in the image.

6 Conclusion

In conclusion, this study aimed to observe ecDNA in the SHEP-2 neuroblastoma cell line, determine the presence and location of DNA within EV isolation fractions, and investigate the potential transfer of EV-associated ecDNA between different cell types.

Metaphase spreads were employed to visualize ecDNA morphology and quantity in SHEP-2 cells. Despite extensive optimization efforts, the inherent complexity of overlapping chromosomal fragments in metaphase spreads posed a significant challenge. The difficulty in distinguishing individual chromosomes hindered a clear observation of ecDNA.

The investigation into EVs secreted by SHEP-2 cells revealed the presence of DNA in the EV fraction, both with and without enzymatic DNA digestion. This suggests the existence of both free or vesicle-associated DNA and membrane-enclosed DNA within the isolation fraction. The EV yield and the exclusion of non-EV material are not evaluated.

In the exploration of ecDNA transfer in cases where the genes are unidentified, we effectively utilized a bioorthogonal metabolic labelling strategy within cells adhering to coverslips. However, the specific detection of ecDNA in the EV fraction remained inconclusive, as the experiment for bioorthogonal metabolically labelled DNA in gel electrophoresis encountered challenges such as fluorophore binding issues or a potential absence of ecDNA in the sample. The experiment designed to explore the transfer of ecDNA through EVs did not yield conclusive results. Despite the lack of findings, this experiment lays the groundwork for future investigations.

This research provides valuable insights into the complexities associated with investigating ecDNA in neuroblastoma cells and its potential packaging within EVs. The findings, limitations, and challenges identified in this study provide a foundation for future research endeavours to the roles played by ecDNA in cellular processes and intercellular communication.

7 Discussion

The initial step driving our investigation was to ascertain the presence of ecDNA in SHEP2 cells. However, this required more optimisation steps than initially anticipated. Despite engaging in the production of numerous metaphase spreads and persistent efforts to optimize the experimental protocol, only a limited number of valuable images were generated. Unfortunately, none of these images could confirm the presence of ecDNA in SHEP2 cells. In hindsight, our results could be consistent with prior research, specifically concerning the far parent cell line of SHEP-2, known as SK-N-SH. This lineage, unlike many other cell lines, was shown in earlier studies to lack any detectable ecDNA content.[86] The study by Biedler et al. provides a compelling reference point, highlighting the ecDNA-free nature of SK-N-SH cells. This observation reinforces the notion that the choice of a cell line is important for the optimisation of the metaphase protocol in the lab. By using cell lines known to harbour ecDNA, we can enhance the relevance and significance of our investigations into the dynamics and implications of ecDNA in EVs. For the detection and counting of ecDNA, when visually detectable, Rajkumar et al.[87] implemented Python code for semantic segmentation of metaphase images containing extrachromosomal DNA. The code was obtained from the author. The segmentation software has not been used here while overlapping DNA structures were abundant in most images.

To enhance the quality of metaphase chromosome spreads, a departure from the conventional cell treatment on coverslips is recommended. Instead, Wu et al. proposed a more effective approach involving the treatment of cells with 75 mM KCl in suspension, as documented in their study.[50] The rationale behind this modification lies in the advantageous absence of cell attachment to a surface, allowing for greater cellular expansion before eventual bursting.

Wu et al.'s research demonstrated the successful visualization of ecDNA through DAPI staining. An alternative technique for identifying ecDNA involves chromosome banding, where these entities manifest as small nonbanding structures, as elucidated by Biedler et al.[86]. In our investigation, we also employed a Fluorescence In Situ Hybridization (FISH)-based method, utilizing MYCN FISH probes to discern amplified oncogenes residing on ecDNAs. Unfortunately, due to an unoptimized protocol or non-functioning FISH probe and the inherent challenge of detecting ecDNA in the SH-EP2 cell line, these results did not contribute to the research question.

Numerous studies have demonstrated successful isolation of intact EVs using differential centrifugation.[88, 76, 77, 12] However, our study introduces a critical question: do we indeed isolate only EVs using the current differential centrifugation protocol? Results from western blot analysis performed by colleagues utilizing an identical EV enrichment protocol showed positive results for EV proteins. To conclude this question further, electron microscopy emerges as a valuable next step. Morphological characterization can confirm the presence of EVs and distinguish them from other cellular debris.

Ultracentrifugation is a widely employed method for EV isolation, yet its efficiency in separating EVs from apoptotic bodies and other small cell debris remains an area of interest. Studies indicate that apoptotic bodies, which share size characteristics with EVs, maybe co-isolated during ultracentrifugation. The observed increase in isolated DNA quantity with prolonged F-ara-Edu incubation aligns with findings in the existing scientific literature regarding the presence of apoptotic bodies in EV fractions. Apoptotic bodies are known to contain fragmented DNA as a consequence of programmed cell death, and their incorporation into EV fractions during the isolation process is a well-documented phenomenon.[89, 88, 64] Western blot analysis for known exosome surface proteins, suchs

as TSG101, HSP70, Alix 1, CD9, CD63, CD81, CD82 and proteins known to be associated with the apoptotic pathway, such as caspases, or proteins associated with the cell cytoskeleton, such as actin or tubulin could be considered a valuable procedure to indicate the quantity of apoptotic bodies and debris of apoptotic origin.

The choice of ultracentrifugation as the method for EV isolation in this research, particularly for DNA quantification, warrants careful consideration. Ultracentrifugation is a well-established and widely used technique that falls within the category of high recovery, low specificity methods. This means it is designed to recover a maximum amount of extracellular material, irrespective of its vesicular or non-vesicular nature. Our study aligns with the broader discussion in the field regarding the trade-off between recovery and specificity in EV isolation methods. While ultracentrifugation provides a high recovery of EVs, the associated challenges, such as buffer effects, potential alterations in EV integrity and co-isolating non-vesicle debris necessitate a critical evaluation of its suitability, especially when focusing on downstream applications like DNA quantification, in which higher specificity is preferred. Methods falling into this category often involve intricate separation strategies based on EV characteristics such as size, density, surface protein/lipid composition, or other biophysical properties. For instance, techniques like size-exclusion chromatography, immunoaffinity isolation, and density gradient ultracentrifugation aim to isolate distinct EV subtypes with minimal contamination from other extracellular materials. While the emphasis on high specificity is critical, it must be noted that there are many potential challenges associated with these methods. One notable challenge is the trade-off between recovery and specificity. High selectivity inherently leads to lower recovery rates, meaning that a substantial fraction of EVs might be excluded during the isolation process. This can pose challenges, especially when the starting material is limited, as it may result in insufficient quantities of isolated EVs for downstream analyses. In this study, the use of substantial volumes for each parameter made the ultracentrifugation process exceptionally time-consuming. Additionally, the effectiveness of high-specificity methods can be influenced by the heterogeneity of EV populations. [64] A logical next experiment would be to include an additional 10000 to 20000 g centrifugation step as stated in chapter 3.1.3 and implemented by Fisher et al., which, according to the research, did not yield any DNA from apoptotic bodies. After validation of this protocol, DNA quantification might yield more representative results.[12]

The use of a hypotonic Tris buffer in the first EV isolation and EV-DNA quantification method affected the DNA yield negatively. Isotonic buffers, such as PBS, are recommended to maintain EV integrity during isolation.It was shown that using low osmolarity buffers, like Tris-HCl, may result in osmotic stress, potentially lysing EVs. This should still be confirmed by advanced imaging techniques for instance electron microscopy.

Different DNA isolation methods can impact the size and yield of extracted DNA. While column separation and phenol-chloroform extraction are common techniques, their implications on the integrity of extracellular DNA are not well-documented. Literature suggests that phenol-chloroform extraction may preserve larger DNA fragments due to reduced shearing during the isolation process. Therefore, in this research, the phenol-chloroform extraction was preferred, while the QIAamp DNA Mini Kit only claims to isolate DNA up to 50 kilobase pairs effectively. When researching larger DNA fragments, this should be taken into consideration.

The large size of ecDNA in neuroblastoma, as discussed in chapter 2, probably in the megabase-pair range, poses challenges for visualization using standard gel electrophoresis. The absence of Cy5 fluorescence binding to DNA in figure 12b suggests potential issues with the reaction conditions or the compatibility of the chosen fluorophore with

the DNA fragments. Further investigations into the CuAAC reaction parameters, choice of cell line, choice of labelling components, and potential interference factors are warranted to refine the method for accurate detection of horizontally transferred DNA. Despite this unexpected result, the retained DNA bands open avenues for additional exploration and optimization of the labelling strategy for a more reliable assessment of horizontal DNA transfer facilitated by extracellular vesicles. Pulse field gel electrophoresis (PFGE) emerges as a suitable technique for separating high molecular weight DNA fragments, providing a more accurate assessment of ecDNA content in EVs. Another concern for the visualisation of ecDNA on a gel is the low concentration in the EV sample. Incorporating biotin-streptavidin labelling, especially in conjunction with F-ara-EdU, presents a possible approach to improve the detectability of DNA in PFGE. Biotin-streptavidin interactions provide a highly specific and strong linkage in which four biotin-linked molecules can bind to one streptavadin-linked molecule, amplifying a signal three-fold and thus enhancing the resolution and visualization of DNA fragments. While knowledge of biotin-steptavadin signal amplification was present within the lab, PFGE was not. This means that this detection method remains a recommendation for the detection of ecDNA in EV samples.

Serum starvation is recognized to induce cellular alterations, influencing diverse cellular processes, including the secretion of EVs. However, the challenge lies in distinguishing the EVs originating from the cells of interest from those present in fetal bovine serum (FBS). Conventional methods, such as ultracentrifugation, are commonly employed to remove EVs from FBS before further analysis. This process has been proposed to reveal distinct EV fractions and their associated DNA contents.[90]. An alternative could be the addition of F-ara-EdU to complete culture media. F-ara-EdU containing DNA can be attached to a photocleavable biotin-azide linker. Subsequent neutravadin affinity purification and cleavage by UV irradiation might yield only EV-DNA originating from the cell nucleus, excluding DNA from the co-isolation of serum-derived EVs. This refined approach could provide a more detailed insight into how cellular conditions, such as serum starvation, impact the DNA cargo and composition of EVs, advancing our understanding of intercellular DNA transfer mediated by these vesicles.

References

1. Yan P, Qi F, Bian L, Xu YD, Zhou JF, Hu JC, Ren LA, Li AFG M, Tang W, and Li M. Comparison of Incidence and Outcomes of Neuroblastoma in Children, Adolescents, and Adults in the United States: A Surveillance, Epidemiology, and End Results (SEER) Program Population Study. 2020. DOI: 10.12659/MSM.927218. Available from: https://www.medscimonit.com/abstract/index/idArt/927218
2. Althoff K, Beckers A, Bell E, Nortmeyer M, Thor T, Sprüssel A, Lindner S, De Preter K, Florin A, Heukamp LC, Klein-Hitpass L, Astrahantseff K, Kumps C, Speleman F, Eggert A, Westermann F, Schramm A, and Schulte JH. A Cre-conditional MYCN-driven neuroblastoma mouse model as an improved tool for preclinical studies. Oncogene 2015 Jun; 34:3357–68. DOI: 10.1038/ONC.2014.269. Available from: https://pubmed.ncbi.nlm.nih.gov/25174395/
3. Lonergan GJ, Schwab CM, Suarez ES, and Carlson CL. Neuroblastoma, ganglioneuroblastoma, and ganglioneuroma: radiologic-pathologic correlation. Radiographics : a review publication of the Radiological Society of North America, Inc 2002; 22:911–34. DOI: 10.1148/RADIOGRAPHICS.22.4.G02JL15911. Available from: https://pubmed.ncbi.nlm.nih.gov/12110723/
4. Siegel Mph RL, Miller KD, Sandeep N, Mbbs W, Ahmedin |, Dvm J, and Siegel RL. Cancer statistics, 2023. CA: A Cancer Journal for Clinicians 2023 Jan; 73:17–48. DOI: 10.3322/CAAC.21763. Available from: https://onlinelibrary.wiley.com/doi/full/10.3322/caac.21763%20https://onlinelibrary.wiley.com/doi/abs/10.3322/caac.21763%20https://acsjournals.onlinelibrary.wiley.com/doi/10.3322/caac.21763
5. Turner KM, Deshpande V, Beyter D, Koga T, Rusert J, Lee C, Li B, Arden K, Ren B, Nathanson DA, Kornblum HI, Taylor MD, Kaushal S, Cavenee WK, Wechsler-Reya R, Furnari FB, Vandenberg SR, Rao PN, Wahl GM, Bafna V, and Mischel PS. Extrachromosomal oncogene amplification drives tumor evolution and genetic heterogeneity. Nature 2017 Mar; 543:122. DOI: 10.1038/NATURE21356. Available from: /pmc/articles/PMC5334176/%20/pmc/articles/PMC5334176/?report=abstract%20https://www.ncbi.nlm.nih.gov/pmc/articles/PMC5334176/
6. Karami Fath M, Karimfar N, Fazlollahpour Naghibi A, Shafa S, Ghasemi Shiran M, Ataei M, Dehghanzadeh H, Nabi Afjadi M, Ghadiri T, Payandeh Z, and Tarhriz V. Revisiting characteristics of oncogenic extrachromosomal DNA as mobile enhancers on neuroblastoma and glioma cancers. Cancer Cell International 2022 22:1 2022 May; 22:1–14. DOI: 10.1186/S12935-022-02617-8. Available from: https://cancerci.biomedcentral.com/articles/10.1186/s12935-022-02617-8
7. Pecorino LT, Verhaak RG, Henssen A, and Mischel PS. Extrachromosomal DNA (ecDNA): an origin of tumor heterogeneity, genomic remodeling, and drug resistance. Biochemical Society Transactions 2022 Dec; 50:1911–20. DOI: 10.1042/BST20221045. Available from: /biochemsoctrans/article/50/6/1911/232076/Extrachromosomal-DNA-ecDNA-an-origin-of-tumor%20https://portlandpress.com/biochemsoctrans/article/50/6/1911/232076/Extrachromosomal-DNA-ecDNA-an-origin-of-tumor
8. Yi E, Chamorro González R, Henssen AG, and Verhaak RGW. Extrachromosomal DNA amplifications in cancer. Nature Reviews Genetics 2022 23:12 2022 Aug; 23:760–71. DOI: 10.1038/s41576-022-00521-5. Available from: https://www.nature.com/articles/s41576-022-00521-5

9. Seeger RC, Brodeur GM, Sather H, Dalton A, Siegel SE, Wong KY, and Hammond D. Association of Multiple Copies of the N-myc Oncogene with Rapid Progression of Neuroblastomas. http://dx.doi.org/10.1056/NEJM198510313131802 1985 Jan; 313:1111–6. DOI: 10.1056/NEJM198510313131802. Available from: https://www.nejm.org/doi/full/10.1056/NEJM198510313131802
10. Huang M and Weiss WA. Neuroblastoma and MYCN. Cold Spring Harbor Perspectives in Medicine 2013; 3. DOI: 10.1101/CSHPERSPECT.A014415. Available from: /pmc/articles/PMC3784814/%20/pmc/articles/PMC3784814/?report=abstract%20https://www.ncbi.nlm.nih.gov/pmc/articles/PMC3784814/
11. Otte J, Dyberg C, Pepich A, and Johnsen JI. MYCN Function in Neuroblastoma Development. Frontiers in Oncology 2021 Jan; 10:3210. DOI: 10.3389/FONC.2020.624079
12. Fischer S, Cornils K, Speiseder T, Badbaran A, Reimer R, Indenbirken D, Grundhoff A, Brunswig-Spickenheier B, Alawi M, and Lange C. Indication of Horizontal DNA Gene Transfer by Extracellular Vesicles. PLoS ONE 2016 Sep; 11. DOI: 10.1371/JOURNAL.PONE.0163665. Available from: /pmc/articles/PMC5042424/%20/pmc/articles/PMC5042424/?report=abstract%20https://www.ncbi.nlm.nih.gov/pmc/articles/PMC5042424/
13. Doyle LM and Wang MZ. Overview of Extracellular Vesicles, Their Origin, Composition, Purpose, and Methods for Exosome Isolation and Analysis. Cells 2019 Jul; 8. DOI: 10.3390/CELLS8070727. Available from: /pmc/articles/PMC6678302/%20/pmc/articles/PMC6678302/?report=abstract%20https://www.ncbi.nlm.nih.gov/pmc/articles/PMC6678302/
14. Jahangiri L and Ishola T. Exosomes in Neuroblastoma Biology, Diagnosis, and Treatment. Life 2022 Nov; 12. DOI: 10.3390/LIFE12111714. Available from: /pmc/articles/PMC9694311/%20/pmc/articles/PMC9694311/?report=abstract%20https://www.ncbi.nlm.nih.gov/pmc/articles/PMC9694311/
15. Marimpietri D, Airoldi I, Faini AC, Malavasi F, and Morandi F. The Role of Extracellular Vesicles in the Progression of Human Neuroblastoma. International Journal of Molecular Sciences 2021 Apr; 22. DOI: 10.3390/IJMS22083964. Available from: /pmc/articles/PMC8069919/%20/pmc/articles/PMC8069919/?report=abstract%20https://www.ncbi.nlm.nih.gov/pmc/articles/PMC8069919/
16. Lange JT, Rose JC, Chen CY, Pichugin Y, Xie L, Tang J, Hung KL, Yost KE, Shi Q, Erb ML, Rajkumar U, Wu S, Taschner-Mandl S, Bernkopf M, Swanton C, Liu Z, Huang W, Chang HY, Bafna V, Henssen AG, Werner B, and Mischel PS. The evolutionary dynamics of extrachromosomal DNA in human cancers. Nature Genetics 2022 54:10 2022 Sep; 54:1527–33. DOI: 10.1038/s41588-022-01177-x. Available from: https://www.nature.com/articles/s41588-022-01177-x
17. Mahapatra S and Challagundla KB. Neuroblastoma. StatPearls 2023 Feb. Available from: https://www.ncbi.nlm.nih.gov/books/NBK448111/
18. London WB, Castleberry RP, Matthay KK, Look AT, Seeger RC, Shimada H, Thorner P, Brodeur G, Maris JM, Reynolds CP, and Cohn SL. Evidence for an age cutoff greater than 365 days for neuroblastoma risk group stratification in the Children's Oncology Group. Journal of Clinical Oncology 2005 Sep; 23:6459–65. DOI: 10.1200/JCO.2005.05.571
19. Thiele C. Neuroblastoma Cell Lines. J. Human Cell Culture 1998 Jan; 1:21–53
20. Matthay KK, Maris JM, Schleiermacher G, Nakagawara A, Mackall CL, Diller L, and Weiss WA. Neuroblastoma. Nature reviews. Disease primers 2016 Nov; 2. DOI: 10.1038/NRDP.2016.78. Available from: https://pubmed.ncbi.nlm.nih.gov/27830764/

21. Finklestein JZ and Gilchrist GS. Recent advances in neuroblastoma. The New England journal of medicine 2010 Mar; 362:116–27. DOI: 10.1056/NEJMRA0804577. Available from: https://pubmed.ncbi.nlm.nih.gov/20558371/

22. Papaioannou G and McHugh K. Neuroblastoma in childhood: review and radiological findings. Cancer Imaging 2005; 5:116. DOI: 10.1102/1470-7330.2005.0104. Available from: /pmc/articles/PMC1665241/%20/pmc/articles/PMC1665241/?report=abstract%20https://www.ncbi.nlm.nih.gov/pmc/articles/PMC1665241/

23. Kushner BH. Neuroblastoma: A Disease Requiring a Multitude of Imaging Studies*. Available from: http://www.snm.org/ce_online

24. Hugosson C, Nyman R, Jorulf H, Mcdonald P, Rifai A, Kofide A, and Jacobsson B. Imaging of abdominal neuroblastoma in children. Acta radiologica (Stockholm, Sweden : 1987) 1999; 40:534–42. DOI: 10.3109/02841859909175580. Available from: https://pubmed.ncbi.nlm.nih.gov/10485244/

25. Heukamp LC, Thor T, Schramm A, De Preter K, Kumps C, De Wilde B, Odersky A, Peifer M, Lindner S, Spruessel A, Pattyn F, Mestdagh P, Menten B, Kuhfittig-Kulle S, Künkele A, König K, Meder L, Chatterjee S, Ullrich RT, Schulte S, Vandesompele J, Speleman F, Büttner R, Eggert A, and Schulte JH. Targeted expression of mutated ALK induces neuroblastoma in transgenic mice. Science translational medicine 2012 Jul; 4. DOI: 10.1126/SCITRANSLMED.3003967. Available from: https://pubmed.ncbi.nlm.nih.gov/22764207/

26. Molenaar JJ, Koster J, Zwijnenburg DA, Van Sluis P, Valentijn LJ, Van Der Ploeg I, Hamdi M, Van Nes J, Westerman BA, Van Arkel J, Ebus ME, Haneveld F, Lakeman A, Schild L, Molenaar P, Stroeken P, Van Noesel MM, Øra I, Santo EE, Caron HN, Westerhout EM, and Versteeg R. Sequencing of neuroblastoma identifies chromothripsis and defects in neuritogenesis genes. Nature 2012 483:7391 2012 Feb; 483:589–93. DOI: 10.1038/nature10910. Available from: https://www.nature.com/articles/nature10910

27. Fransson S, Martinez-Monleon A, Johansson M, Sjöberg RM, Björklund C, Ljungman G, Ek T, Kogner P, and Martinsson T. Whole-genome sequencing of recurrent neuroblastoma reveals somatic mutations that affect key players in cancer progression and telomere maintenance. Scientific Reports 2020 Dec; 10. DOI: 10.1038/S41598-020-78370-7. Available from: /pmc/articles/PMC7775426/%20/pmc/articles/PMC7775426/?report=abstract%20https://www.ncbi.nlm.nih.gov/pmc/articles/PMC7775426/

28. Cellosaurus cell line Tet2 (CVCL_HF70). Available from: https://www.cellosaurus.org/CVCL_HF70

29. Cellosaurus cell line SK-N-SH (CVCL_0531). Available from: https://www.cellosaurus.org/CVCL_0531

30. Kryh H, Carén H, Erichsen J, Sjöberg RM, Abrahamsson J, Kogner P, and Martinsson T. Comprehensive SNP array study of frequently used neuroblastoma cell lines; copy neutral loss of heterozygosity is common in the cell lines but uncommon in primary tumors. BMC Genomics 2011 Sep; 12:1–11. DOI: 10.1186/1471-2164-12-443/FIGURES/4. Available from: https://bmcgenomics.biomedcentral.com/articles/10.1186/1471-2164-12-443

31. ALK (anaplastic lymphoma receptor tyrosine kinase). Available from: https://atlasgeneticsoncology.org/gene/16/alk-(anaplastic-lymphoma-receptor-tyrosine-kinase)

32. NRAS (neuroblastoma RAS viral oncogene homolog). Available from: https://atlasgeneticsoncology.org/gene/92/nras-(neuroblastoma-ras-viral-oncogene-homolog)

33. W Verhaak RG, Bafna V, and Mischel PS. Extrachromosomal oncogene amplification in tumour pathogenesis and evolution. Nature Reviews Cancer. DOI: 10.1038/s41568-019-0128-6. Available from: www.nature.com/nrc

34. Decarvalho AC, Kim H, Poisson LM, Winn ME, Mueller C, Cherba D, Koeman J, Seth S, Protopopov A, Felicella M, Zheng S, Multani A, Jiang Y, Zhang J, Nam DH, Petricoin EF, Chin L, Mikkelsen T, and Verhaak RG. Discordant inheritance of chromosomal and extrachromosomal DNA elements contributes to dynamic disease evolution in glioblastoma. Nature genetics 2018 May; 50:708. DOI: 10.1038/S41588-018-0105-0. Available from: /pmc/articles/PMC5934307/%20/pmc/articles/PMC5934307/?report=abstract%20https://www.ncbi.nlm.nih.gov/pmc/articles/PMC5934307/

35. Koche RP, Rodriguez-Fos E, Helmsauer K, Torrents D, Schulte JH, Henssen AG, Burkert M, Macarthur IC, Maag J, Chamorro R, Munoz-Perez N, Puiggròs M, Dorado Garcia H, Bei Y, Röefzaad C, Bardinet V, Szymansky A, Winkler A, Thole T, Timme N, Kasack K, Fuchs S, Klironomos F, Thiessen N, Blanc E, Schmelz K, Künkele A, Hundsdörfer P, Rosswog C, Theissen J, Beule D, Deubzer H, Sauer S, Toedling J, Fischer M, Hertwig F, Schwarz RF, and Eggert A. Extrachromosomal circular DNA drives oncogenic genome remodeling in neuroblastoma. Nature Genetics. DOI: 10.1038/s41588-019-0547-z. Available from: https://doi.org/10.1038/s41588-019-0547-z

36. Kim H, Nguyen NP, Turner K, Wu S, Gujar AD, Luebeck J, Liu J, Deshpande V, Rajkumar U, Namburi S, Amin SB, Yi E, Menghi F, Schulte JH, Henssen AG, Chang HY, Beck CR, Mischel PS, Bafna V, and Verhaak RG. Extrachromosomal DNA is associated with oncogene amplification and poor outcome across multiple cancers. Nature genetics 2020 Sep; 52:891. DOI: 10.1038/S41588-020-0678-2. Available from: /pmc/articles/PMC7484012/%20/pmc/articles/PMC7484012/?report=abstract%20https://www.ncbi.nlm.nih.gov/pmc/articles/PMC7484012/

37. Li Y, Roberts ND, Wala JA, Shapira O, Schumacher SE, Kumar K, Khurana E, Waszak S, Korbel JO, Haber JE, Imielinski M, Akdemir KC, Alvarez EG, Baez-Ortega A, Beroukhim R, Boutros PC, Bowtell DD, Brors B, Burns KH, Campbell PJ, Chan K, Chen K, Cortés-Ciriano I, Dueso-Barroso A, Dunford AJ, Edwards PA, Estivill X, Etemadmoghadam D, Feuerbach L, Fink JL, Frenkel-Morgenstern M, Garsed DW, Gerstein M, Gordenin DA, Haan D, Haber JE, Hess JM, Hutter B, Imielinski M, Jones DT, Ju YS, Kazanov MD, Klimczak LJ, Koh Y, Korbel JO, Kumar K, Lee EA, Lee JJK, Li Y, Lynch AG, Macintyre G, Markowetz F, Martincorena I, Martinez-Fundichely A, Meyerson M, Miyano S, Nakagawa H, Navarro FC, Ossowski S, Park PJ, Pearson JV, Puiggròs M, Rippe K, Roberts ND, Roberts SA, Rodriguez-Martin B, Schumacher SE, Scully R, Shackleton M, Sidiropoulos N, Sieverling L, Stewart C, Torrents D, Tubio JM, Villasante I, Waddell N, Wala JA, Weischenfeldt J, Yang L, Yao X, Yoon SS, Zamora J, Zhang CZ, Weischenfeldt J, and Beroukhim R. Patterns of somatic structural variation in human cancer genomes. Nature 2020 578:7793 2020 Feb; 578:112–21. DOI: 10.1038/s41586-019-1913-9. Available from: https://www.nature.com/articles/s41586-019-1913-9

38. Hadi K, Yao X, Behr JM, Deshpande A, Xanthopoulakis C, Tian H, Kudman S, Rosiene J, Darmofal M, DeRose J, Mortensen R, Adney EM, Shaiber A, Gajic Z, Sigouros M, Eng K, Wala JA, Wrzeszczyński KO, Arora K, Shah M, Emde AK, Felice V, Frank MO, Darnell RB, Ghandi M, Huang F, Dewhurst S, Maciejowski J, Lange T de, Setton J, Riaz N, Reis-Filho JS, Powell S, Knowles DA, Reznik E, Mishra B, Beroukhim R, Zody MC, Robine N, Oman KM, Sanchez CA, Kuhner MK, Smith LP, Galipeau PC, Paulson TG, Reid BJ, Li X, Wilkes D, Sboner A, Mosquera JM, Elemento O, and Imielinski M. Distinct classes of complex structural variation uncovered across thousands of cancer genome graphs. Cell 2020 Oct; 183:197. DOI: 10.1016/J.CELL.2020.08.006.

Available from: /pmc/articles/PMC7912537/%20/pmc/articles/PMC7912537/?report=abstract%20https://www.ncbi.nlm.nih.gov/pmc/articles/PMC7912537/

39. Zhao Y, Yu L, Zhang S, Su X, and Zhou X. Extrachromosomal circular DNA: Current status and future prospects. eLife 2022; 11. DOI: 10.7554/ELIFE.81412. Available from: /pmc/articles/PMC9578701/%20/pmc/articles/PMC9578701/?report=abstract%20https://www.ncbi.nlm.nih.gov/pmc/articles/PMC9578701/

40. Zhang CZ, Spektor A, Cornils H, Francis JM, Jackson EK, Liu S, Meyerson M, and Pellman D. Chromothripsis from DNA damage in micronuclei. Nature 2015 Jun; 522:179–84. DOI: 10.1038/NATURE14493. Available from: https://pubmed.ncbi.nlm.nih.gov/26017310/%20https://pubmed.ncbi.nlm.nih.gov/26017310/?dopt=Abstract

41. Ly P, Brunner SF, Shoshani O, Kim DH, Lan W, Pyntikova T, Flanagan AM, Behjati S, Page DC, Campbell PJ, and Cleveland DW. Chromosome segregation errors generate a diverse spectrum of simple and complex genomic rearrangements. Nature genetics 2019 Apr; 51:705–15. DOI: 10.1038/S41588-019-0360-8. Available from: https://pubmed.ncbi.nlm.nih.gov/30833795/

42. Tang S, Stokasimov E, Cui Y, and Pellman D. Breakage of cytoplasmic chromosomes by pathological DNA base excision repair. Nature 2022 606:7916 2022 Apr; 606:930–6. DOI: 10.1038/s41586-022-04767-1. Available from: https://www.nature.com/articles/s41586-022-04767-1

43. Hatch EM, Fischer AH, Deerinck TJ, and Hetzer MW. Catastrophic nuclear envelope collapse in cancer cell micronuclei. Cell 2013 Jul; 154:47. DOI: 10.1016/J.CELL.2013.06.007. Available from: /pmc/articles/PMC3749778/%20/pmc/articles/PMC3749778/?report=abstract%20https://www.ncbi.nlm.nih.gov/pmc/articles/PMC3749778/

44. Wu S, Bafna V, Chang HY, and Mischel PS. Extrachromosomal DNA: An Emerging Hallmark in Human Cancer. Annual review of pathology 2022 Jan; 17:367. DOI: 10.1146/ANNUREV-PATHMECHDIS-051821-114223. Available from: /pmc/articles/PMC9125980/%20/pmc/articles/PMC9125980/?report=abstract%20https://www.ncbi.nlm.nih.gov/pmc/articles/PMC9125980/

45. Carroll SM, Derose ML, Gaudray P, Charleen Moore IM, Needham-vandevanter DR, Von Hoff DD, Wahl GM, Gaudray P, DeRose ML, Emery JF, Meinkoth JL, Nakkim E, Subler M, Von Hoff DD, and Wahl GM. Double minute chromosomes can be produced from precursors derived from a chromosomal deletion. Molecular and Cellular Biology 1988 Apr; 8:1525. DOI: 10.1128/MCB.8.4.1525. Available from: /pmc/articles/PMC363312/?report=abstract%20https://www.ncbi.nlm.nih.gov/pmc/articles/PMC363312/

46. Guérin TM and Marcand S. Breakage in breakage-fusion-bridge cycle: an 80-year-old mystery. Trends in Genetics 2022; 38:641–5. DOI: 10.1016/j.tig.2022.03.008

47. Maciejowski J, Li Y, Bosco N, Campbell PJ, and De Lange T. Chromothripsis and Kataegis Induced by Telomere Crisis. Cell 2015 Dec; 163:1641–54. DOI: 10.1016/J.CELL.2015.11.054

48. Wang T, Zhang H, Zhou Y, and Shi J. Extrachromosomal circular DNA: a new potential role in cancer progression. Journal of Translational Medicine 2021 19:1 2021 Jun; 19:1–16. DOI: 10.1186/S12967-021-02927-X. Available from: https://translational-medicine.biomedcentral.com/articles/10.1186/s12967-021-02927-x

49. Ottaviani D, LeCain M, and Sheer D. The role of microhomology in genomic structural variation. Trends in Genetics 2014 Mar; 30:85–94. DOI: 10.1016/J.TIG.2014.01.001

50. Wu S, Turner KM, Nguyen N, Raviram R, Erb M, Santini J, Luebeck J, Rajkumar U, Diao Y, Li B, Zhang W, Jameson N, Corces MR, Granja JM, Chen X, Coruh C, Abnousi A, Houston J, Ye Z, Hu R, Yu M, Kim H, Law JA, Verhaak RG, Hu M, Furnari FB, Chang HY, Ren B, Bafna V, and Mischel PS. Circular ecDNA promotes accessible chromatin and high oncogene expression. Nature 2019 Nov; 575:699. DOI: 10.1038/S41586-019-1763-5. Available from: /pmc/articles/PMC7094777/%20/pmc/articles/PMC7094777/?report=abstract%20https://www.ncbi.nlm.nih.gov/pmc/articles/PMC7094777/

51. Zhu Y, Gujar AD, Wong CH, Tjong H, Ngan CY, Gong L, Chen YA, Kim H, Liu J, Li M, Mil-Homens A, Maurya R, Kuhlberg C, Sun F, Yi E, deCarvalho AC, Ruan Y, Verhaak RG, and Wei CL. Oncogenic Extrachromosomal DNA Functions as Mobile Enhancers to Globally Amplify Chromosomal Transcription. Cancer cell 2021 May; 39:694. DOI: 10.1016/J.CCELL.2021.03.006. Available from: /pmc/articles/PMC8119378/%20/pmc/articles/PMC8119378/?report=abstract%20https://www.ncbi.nlm.nih.gov/pmc/articles/PMC8119378/

52. Morton AR, Dogan-Artun N, Faber ZJ, MacLeod G, Bartels CF, Piazza MS, Allan KC, Mack SC, Wang X, Gimple RC, Wu Q, Rubin BP, Shetty S, Angers S, Dirks PB, Sallari RC, Lupien M, Rich JN, and Scacheri PC. Functional enhancers shape extrachromosomal oncogene amplifications. Cell 2019 Nov; 179:1330. DOI: 10.1016/J.CELL.2019.10.039. Available from: /pmc/articles/PMC7241652/%20/pmc/articles/PMC7241652/?report=abstract%20https://www.ncbi.nlm.nih.gov/pmc/articles/PMC7241652/

53. Shimizu N, Itoh N, Utiyama H, and Wahl GM. Selective entrapment of extrachromosomally amplified DNA by nuclear budding and micronucleation during S phase. The Journal of cell biology 1998 Mar; 140:1307–20. DOI: 10.1083/JCB.140.6.1307. Available from: https://pubmed.ncbi.nlm.nih.gov/9508765/

54. Itoh N and Shimizu N. DNA replication-dependent intranuclear relocation of double minute chromatin. Journal of cell science 1998 Nov; 111 (Pt 22):3275–85. DOI: 10.1242/JCS.111.22.3275. Available from: https://pubmed.ncbi.nlm.nih.gov/9788870/

55. Kanda T, Otter M, and Wahl GM. Mitotic segregation of viral and cellular acentric extrachromosomal molecules by chromosome tethering. Journal of Cell Science 2001 Jan; 114:49–58. DOI: 10.1242/JCS.114.1.49. Available from: https://journals.biologists.com/jcs/article/114/1/49/26563/Mitotic-segregation-of-viral-and-cellular-acentric

56. KL H, KE Y, L X, Q S, K H, J L, R S, JT L, R CG, NE W, C C, ME V, IT W, S W, SR D, CV D, K K, J T, JA B, JC R, MR C, JM G, R L, U R, J F, A B, AT S, R T, S M, V B, AG H, PS M, Z L, and HY C. ecDNA hubs drive cooperative intermolecular oncogene expression. Nature 2021; 600. DOI: 10.1038/S41586-021-04116-8. Available from: https://pubmed.ncbi.nlm.nih.gov/34819668/

57. Purshouse K, Friman ET, Boyle S, Dewari PS, Grant V, Hamdan A, Morrison GM, Brennan PM, Beentjes SV, Pollard SM, and Bickmore WA. Oncogene expression from extrachromosomal DNA is driven by copy number amplification and does not require spatial clustering. bioRxiv 2022 Jan :2022.01.29.478046. DOI: 10.1101/2022.01.29.478046. Available from: https://www.biorxiv.org/content/10.1101/2022.01.29.478046v1%20https://www.biorxiv.org/content/10.1101/2022.01.29.478046v1.abstract

58. Helmsauer K, Valieva ME, Ali S, Chamorro González R, Schöpflin R, Röefzaad C, Bei Y, Dorado Garcia H, Rodriguez-Fos E, Puiggròs M, Kasack K, Haase K, Keskeny C, Chen CY, Kuschel LP, Euskirchen P, Heinrich V, Robson MI, Rosswog C, Toedling J, Szymansky A, Hertwig F, Fischer M, Torrents D, Eggert A, Schulte JH, Mundlos S, Henssen AG, and Koche RP. Enhancer hijacking determines extrachromosomal circular MYCN amplicon architecture in neuroblastoma. DOI: 10.1038/s41467-020-19452-y. Available from: https://doi.org/10.1038/s41467-020-19452-y

59. Verhaak RG, Bafna V, and Mischel PS. Extrachromosomal Oncogene Amplification in Tumor Pathogenesis and Evolution. Nature reviews. Cancer 2019 May; 19:283. DOI: 10.1038/S41568-019-0128-6. Available from: /pmc/articles/PMC7168519/%20/pmc/articles/PMC7168519/?report=abstract%20https://www.ncbi.nlm.nih.gov/pmc/articles/PMC7168519/

60. Teng F and Fussenegger M. Shedding Light on Extracellular Vesicle Biogenesis and Bioengineering. Advanced Science 2021 Jan; 8:2003505. DOI: 10.1002/ADVS.202003505. Available from: https://onlinelibrary.wiley.com/doi/full/10.1002/advs.202003505%20https://onlinelibrary.wiley.com/doi/abs/10.1002/advs.202003505%20https://onlinelibrary.wiley.com/doi/10.1002/advs.202003505

61. György B, Szabó TG, Pásztói M, Pál Z, Misják P, Aradi B, László V, Pállinger É, Pap E, Kittel Á, Nagy G, Falus A, and Buzás EI. Membrane vesicles, current state-of-the-art: emerging role of extracellular vesicles. Cellular and molecular life sciences : CMLS 2011 Aug; 68:2667–88. DOI: 10.1007/S00018-011-0689-3. Available from: https://pubmed.ncbi.nlm.nih.gov/21560073/

62. Lane RE, Korbie D, Hill MM, and Trau M. Extracellular vesicles as circulating cancer biomarkers: opportunities and challenges. Clinical and Translational Medicine 2018 Dec; 7:e14. DOI: 10.1186/S40169-018-0192-7. Available from: https://onlinelibrary.wiley.com/doi/full/10.1186/s40169-018-0192-7%20https://onlinelibrary.wiley.com/doi/abs/10.1186/s40169-018-0192-7%20https://onlinelibrary.wiley.com/doi/10.1186/s40169-018-0192-7

63. Van Niel G, D'Angelo G, and Raposo G. Shedding light on the cell biology of extracellular vesicles. Nature Reviews Molecular Cell Biology 2018 19:4 2018 Jan; 19:213–28. DOI: 10.1038/nrm.2017.125. Available from: https://www.nature.com/articles/nrm.2017.125

64. Théry C et al. Minimal information for studies of extracellular vesicles 2018 (MISEV2018): a position statement of the International Society for Extracellular Vesicles and update of the MISEV2014 guidelines. Journal of Extracellular Vesicles 2018 Jan; 7. DOI: 10.1080/20013078.2018.1535750. Available from: /pmc/articles/PMC6322352/%20/pmc/articles/PMC6322352/?report=abstract%20https://www.ncbi.nlm.nih.gov/pmc/articles/PMC6322352/

65. Cocucci E and Meldolesi J. Ectosomes and exosomes: shedding the confusion between extracellular vesicles. Trends in cell biology 2015 Jun; 25:364–72. DOI: 10.1016/J.TCB.2015.01.004. Available from: https://pubmed.ncbi.nlm.nih.gov/25683921/

66. Gould SJ and Raposo G. As we wait: coping with an imperfect nomenclature for extracellular vesicles. Journal of extracellular vesicles 2013; 2. DOI: 10.3402/JEV.V2I0.20389. Available from: https://pubmed.ncbi.nlm.nih.gov/24009890/

67. OBrien K, Breyne K, Ughetto S, Laurent LC, and Breakefield XO. RNA delivery by extracellular vesicles in mammalian cells and its applications. Nature Reviews Molecular Cell Biology. DOI: 10.1038/s41580-020-0251-y. Available from: www.nature.com/nrm

68. C K, SA M, A P, J T, S S, M K, J Z, J W, L C, A F, and R K. Identification of double-stranded genomic DNA spanning all chromosomes with mutated KRAS and p53 DNA in the serum exosomes of patients with pancreatic cancer. The Journal of biological chemistry 2014; 289. DOI: 10.1074/JBC.C113.532267. Available from: https://pubmed.ncbi.nlm.nih.gov/24398677/

69. BK T, H Z, A B, I M, Y H, B CS, Y Z, A H, H B, J X, C W, R RB, JM S, W Z, S H, O E, N P, K MT, K W, J B, H P, and D L. Double-stranded DNA in exosomes: a novel biomarker in cancer detection. Cell research 2014; 24. DOI: 10.1038/CR.2014.44. Available from: https://pubmed.ncbi.nlm.nih.gov/24710597/

70. Ghanam J, Chetty VK, Barthel L, Reinhardt D, Hoyer PF, and Thakur BK. DNA in extracellular vesicles: from evolution to its current application in health and disease. Cell & Bioscience 2022 12:1 2022 Mar; 12:1–13. DOI: 10.1186/S13578-022-00771-0. Available from: https://cellandbioscience.biomedcentral.com/articles/10.1186/s13578-022-00771-0

71. Ciferri MC, Quarto R, and Tasso R. Extracellular Vesicles as Biomarkers and Therapeutic Tools: From Pre-Clinical to Clinical Applications. Biology 2021; 10. DOI: 10.3390/BIOLOGY10050359. Available from: /pmc/articles/PMC8145169/%20/pmc/articles/PMC8145169/?report=abstract%20https://www.ncbi.nlm.nih.gov/pmc/articles/PMC8145169/

72. Balaj L, Lessard R, Dai L, Cho YJ, Pomeroy SL, Breakefield XO, and Skog J. Tumour microvesicles contain retrotransposon elements and amplified oncogene sequences. Nature Communications 2011 2:1 2011 Feb; 2:1–9. DOI: 10.1038/ncomms1180. Available from: https://www.nature.com/articles/ncomms1180

73. Guescini M, Susanna AE, Ae G, Stocchi V, Luigi AE, and Agnati F. Astrocytes and Glioblastoma cells release exosomes carrying mtDNA. DOI: 10.1007/s00702-009-0288-8

74. Krylova SV and Feng D. The Machinery of Exosomes: Biogenesis, Release, and Uptake. International Journal of Molecular Sciences 2023; 24. DOI: 10.3390/IJMS24021337. Available from: /pmc/articles/PMC9865891/%20/pmc/articles/PMC9865891/?report=abstract%20https://www.ncbi.nlm.nih.gov/pmc/articles/PMC9865891/

75. Gurung S, Perocheau D, Touramanidou L, and Baruteau J. The exosome journey: from biogenesis to uptake and intracellular signalling. Cell Communication and Signaling 2021 19:1 2021 Apr; 19:1–19. DOI: 10.1186/S12964-021-00730-1. Available from: https://biosignaling.biomedcentral.com/articles/10.1186/s12964-021-00730-1

76. Zhang M, Jin K, Gao L, Zhang Z, Li F, Zhou F, and Zhang L. Methods and Technologies for Exosome Isolation and Characterization. Small Methods 2018 Sep; 2:1800021. DOI: 10.1002/SMTD.201800021. Available from: https://onlinelibrary.wiley.com/doi/full/10.1002/smtd.201800021%20https://onlinelibrary.wiley.com/doi/abs/10.1002/smtd.201800021%20https://onlinelibrary.wiley.com/doi/10.1002/smtd.201800021

77. Akbar A, Malekian F, Baghban N, Kodam SP, and Ullah M. Methodologies to Isolate and Purify Clinical Grade Extracellular Vesicles for Medical Applications. Cells 2022; 11. DOI: 10.3390/CELLS11020186. Available from: /pmc/articles/PMC8774122/%20/pmc/articles/PMC8774122/?report=abstract%20https://www.ncbi.nlm.nih.gov/pmc/articles/PMC8774122/

78. Salih M, Zietse R, and Hoorn EJ. Urinary extracellular vesicles and the kidney: biomarkers and beyond. American journal of physiology. Renal physiology 2014 Jun; 306. DOI: 10.1152/AJPRENAL.00128.2014. Available from: https://pubmed.ncbi.nlm.nih.gov/24694589/

79. Neef AB and Luedtke NW. Dynamic metabolic labeling of DNA in vivo with arabinosyl nucleosides. Proceedings of the National Academy of Sciences of the United States of America 2011; 108. DOI: 10.1073/pnas.1101126108

80. Zhu L, Brassard CJ, Zhang X, Guha PM, and Clark RJ. On the Mechanism of Copper(I)-Catalyzed Azide–Alkyne Cycloaddition. The Chemical Record 2016 Jun; 16:1501–17. DOI: 10.1002/TCR.201600002. Available from: https://onlinelibrary.wiley.com/doi/full/10.1002/tcr.201600002%20https://onlinelibrary.wiley.com/doi/abs/10.1002/tcr.201600002%20https://onlinelibrary.wiley.com/doi/10.1002/tcr.201600002

81. Fantoni Z, El-Sagheer AH, and Brown T. A Hitchhiker's Guide to Click-Chemistry with Nucleic Acids. 2021. DOI: 10.1021/acs.chemrev.0c00928. Available from: https://dx.doi.org/10.1021/acs.chemrev.0c00928

82. Huisgen R. 1,3-Dipolar Cycloadditions. Past and Future. Angewandte Chemie International Edition in English 1963 Oct; 2:565–98. DOI: 10.1002/ANIE.196305651. Available from: https://onlinelibrary.wiley.com/doi/full/10.1002/anie.196305651%20https://onlinelibrary.wiley.com/doi/abs/10.1002/anie.196305651%20https://onlinelibrary.wiley.com/doi/10.1002/anie.196305651

83. Gothelf KV and Jørgensen KA. Asymmetric Reactions. *Synthetic Applications of 1,3-Dipolar Cycloaddition Chemistry Toward Heterocycles and Natural Products*. Chemistry of Heterocyclic Compounds: A Series Of Monographs. 2002 Apr :817–99. DOI: https://doi.org/10.1002/0471221902.ch12. Available from: https://doi.org/10.1002/0471221902.ch12

84. Himo F, Lovell T, Hilgraf R, Rostovtsev VV, Noodleman L, Sharpless KB, and Fokin VV. Copper(I)-catalyzed synthesis of azoles. DFT study predicts unprecedented reactivity and intermediates. Journal of the American Chemical Society 2005 Jan; 127:210–6. DOI: 10.1021/ja0471525

85. Besanceney-Webler C, Jiang H, Zheng T, Feng L, Amo DSd, Wang W, Klivansky LM, Marlow PDFL, Liu DY, and Wu PDP. Raising the Efficacy of Bioorthogonal Click Reactions for Bioconjugation: A Comparative Study. Angewandte Chemie (International ed. in English) 2011 Aug; 50:8051. DOI: 10.1002/ANIE.201101817. Available from: /pmc/articles/PMC3465470/%20https://www.ncbi.nlm.nih.gov/pmc/articles/PMC3465470/

86. Biedler JL, Meyers MB, and Spengler BA. Homogeneously Staining Regions and Double Minute Chromosomes, Prevalent Cytogenetic Abnormalities of Human Neuroblastoma Cells. Vol. 4. Elsevier, 1983 Jan :267–307. DOI: 10.1016/B978-0-12-008304-6.50015-4. Available from: https://linkinghub.elsevier.com/retrieve/pii/B9780120083046500154

87. Rajkumar U, Turner K, Luebeck J, Deshpande V, Chandraker M, Mischel P, and Bafna V. EcSeg: Semantic Segmentation of Metaphase Images Containing Extrachromosomal DNA. iScience 2019; 21. DOI: 10.1016/j.isci.2019.10.035

88. Chen D, Zhao Z, Zhang K, Jin F, Zheng C, and Jin Y. Protocol for differential centrifugation-based separation and characterization of apoptotic vesicles derived from human mesenchymal stem cells. STAR Protocols 2022 Dec; 3:101695. DOI: 10.1016/J.XPRO.2022.101695. Available from: /pmc/articles/PMC9494288/%20/pmc/articles/PMC9494288/?report=abstract%20https://www.ncbi.nlm.nih.gov/pmc/articles/PMC9494288/

89. Caruso S and Poon IKH. Apoptotic Cell-Derived Extracellular Vesicles: More Than Just Debris. Frontiers in Immunology 2018; 9. DOI: 10.3389/FIMMU.2018.01486. Available from: /pmc/articles/PMC6031707/%20/pmc/articles/PMC6031707/?report=abstract%20https://www.ncbi.nlm.nih.gov/pmc/articles/PMC6031707/

90. Lehrich BM, Liang Y, Khosravi P, Federoff HJ, and Fiandaca MS. Fetal bovine serum-derived extracellular vesicles persist within vesicle-depleted culture media. International Journal of Molecular Sciences 2018; 19. DOI: 10.3390/ijms19113538